Study of interface delamination in uni-directional CFRP laminate under static loading condition: Experiments and cohesive zone modelling

Sukanya Pravin Joshi

A Thesis Submitted to

Indian Institute of Technology Hyderabad

In Partial Fulfillment of the Requirements for

The Degree of Master of Technology

भारतीय प्रौद्योगिकी संस्थान हैदराबाद

Indian Institute of Technology Hyderabad

Department of Mechanical and Aerospace Engineering

June 2016

Declaration

I declare that this written submission represents my ideas in my own words, and where ideas or words of others have been included, I have adequately cited and referenced the original sources. I also declare that I have adhered to all principles of academic honesty and integrity and have not misrepresented or fabricated or falsified any idea/data/fact/source in my submission. I understand that any violation of the above will be a cause for disciplinary action by the Institute and can also evoke penal action from the sources that have thus not been properly cited, or from whom proper permission has not been taken when needed.

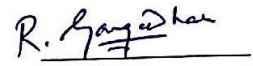(Signature)

Sukanya Pravin Joshi

(Sukanya Pravin Joshi)

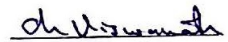ME14MTECH11037

(Roll No.)

Approval Sheet

This Thesis entitled Study of interface delamination in uni-directional CFRP laminate under static loading condition: Experiments and cohesive zone modelling by Sukanya Pravin Joshi is approved for the degree of Master of Technology from IIT Hyderabad

(Dr. Gangadharan) Examiner
Dept. of Mechanical and Aerospace engineering
IITH

(Dr. Syed) Examiner
Dept. of Mechanical and Aerospace engineering
IITH

(Dr. Viswanath Chinthapenta) Adviser
Dept. Mechanical and Aerospace engineering
IITH

(Dr. Suriya) Chairman
Dept. of Civil Engineering
IITH

Acknowledgements

Dedicated to my late grandmother Maina Joshi

Abstract

Interface delamination is reported to be the dominant mode of failure in the stepped lap joints in CFRP composites. The load transfer between the patch and panel takes place through thin adhesive layer. And it being weak link makes it prone to damages. However, not much work was reported in literature to understand the complex mixed-mode delamination of adhesive layer in CFRP laminates. Our study aims at modelling mixed-mode delamination under quasi-static loading conditions for single and double stepped lap unidirectional CFRP composite joint. Modified Cohesive mode-1 Crack and Mixed mode cohesive zone modelling developed by Benzeggagh and Kanane (1995) are used to model the ductile adhesive failure. The mode-1 and 2 fracture toughness required for Beneggagh-Kanane model are obtained through standard experiments. We calibrated the numerical DCB under opening mode loading with the cohesive crack (in method-1) and the mixed mode delamination (method-2) to obtain the cohesive crack length and mixed mode parameter. Through the calibration we showed that the mixed-mode delmaination modelling can be either modelled using the modified cohesive crack or Benzeggagh-Kanane model. The calibrated quantities is used in understnading the single and double stepped lap joint. Modified cohesive crack is superior of Benzeggagh-Kanane model in estimating the damage intiation load and ultimate failure load.

Contents

List of Figures

List of Tables

Chapter 1

Introduction

1.1 Overview

From the last decade, the use of composites is increasing in the various industries where high performance materials are recommended [1]. Composites have applications in various areas such as aeronautical, automotive, marine, construction, sports equipment etc. The individual components of a composite remain separate and distinct within the structure, but together they act as one. The properties of composites are superior as compared to its individual material from which they are formed. The structural advantage of these materials lie in their high strength and stiffness to weight ratios compared to the metals [2].

Amongst, several types of composites, laminated composites are widely used in thin structures due to their high suitablilty [2]. Laminated composites consist of layers i.e. laminae that are bonded together with thin layers of adhesives. Within a lamina, high strength fibers are combined with a light weight matrix. By selecting sequence of laminae with various orientations of principal material directions, a wide range of mechanical properties of the laminated composites can be tailored.

1.1.1 Failure in composites

To promote the potential strength of composites, it is very important to study the failure mechanisms in detail. There are two types of physical failures that occur in laminated composites and they are intra-laminar and inter-laminar failures. Intra-laminar failures deal with the micro-mechanical components of lamina and include the damages within the lamina such as matrix cracking and fibre breakage in tension and compression. This involves the degradation of in-plane material properties of the lamina. Inter-laminar failures deal with the damages between the two laminae such as delamination. The possibility of failure occurring in composites limits the usage of composites [3, 4]. Structural failure in composite is caused by the evolution of different types of damage mechanisms, such as matrix transverse cracking, fibre failure, fibre/matrix debonding, fibre pull-out and delamination as shown in Fig 1.1. Amongst all the damage mecahnisms, the tensile rupture due to cracking of fibre and matrix and delamination are the most dominant in laminated composites [5]. However, interaction between different damage mechanisms is often observed. This makes the failure analysis of composites difficult. In the present work we focus mostly on the delamination without directly modelling the other damage mechanism. However, their affect is mansifested in form mode mixity.

And in the delamination process due to interactions with other mechanisms, it is observed that fibre pull-out occurs due to weak adhesive bonding between the fibres and polymer matrix.
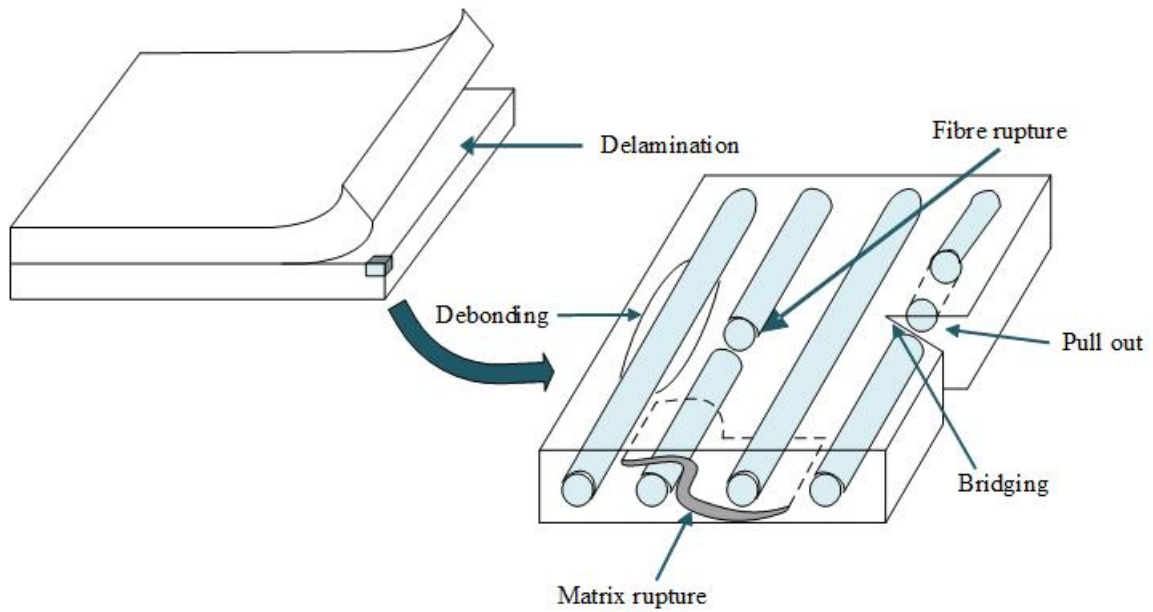
Figure 1.1: Different types of damages in composite

Delamination is the failure of interface between the adjacent laminae and it occurs due to lack of through the thickness reinforcement[3]. Delamination occurs due to several reasons such as high in-service loading, impacts, edge effects, manufacturing defects or high stress concentration at the geometrical or material discontinuities[5, 6, 7]. If damaged area in the component is neglected, the initial delamination associated with it grows and results in degradation of material performance and ultimately leads to component failure. Delamination growth mechanism depends on the initial delamination configuration, inter-facial strength and type of loading causing the separation between the laminae. The loading and boundary conditions of laminated composite structure in structural applications are complex and thus delamination process, in general, becomes mixed-mode phenomena [8]. The delamination is a material response of an interface. Experimental methods to determine inter-facial response under combination loads are time consuming and expensive.

Failure analysis through FEM is useful to technique to predict the behaviour of composites. Delamination is the dominant failure in composite structures and to model damage appropriate damage model has to be established a priori. In general an energy based failure damage mechanism approach is often used to model damage. Damage mechanics deals with the modelling of the damage of material to predict the initiation, propagation, and fracture of materials. It describes the evolution of degradation phenomena from initial state up to separation of the material in the element. This approach is based on the concept of cohesive zone model. In this thesis, formulation of the cohesive zone element is based on the damage model presented by Turon [4]. This formulation is used to study the delamination of adhesive joints in CFRP laminate.

1.2 Literature review on cohesive zone modelling

Delamination is a critical failure mechanism in composites. The model which will predict delamination onset and growth was needed to be developed. Initially delamination growth analysis was performed using fracture mechanics approach. This method requires pre-existing crack with a sharp tip within a material for crack initiation [5]. Therefore the alternative approach of cohesive zone law to describe failure characteristics was introduced. The cohesive zone concept was developed by Dugdale and Barenblatt to describe the fracture process more realistically in metals, such that stress singularities found in LEFM, do not arise [9]. In this method, the crack is divided into two parts: physical crack and cohesive zone. Cohesive zone consists of two cohesive surfaces which are held together by traction. Cohesive zone law is a phenomenological constitutive relation that describes separation along cohesive surfaces. The concept of cohesive zone model has been used to examine different material failure phenomena such as delamination [1, 5], particle debonding [10], matrix decohesion [11], dynamic fracture [12], multiple cracks in brittle materials [13].

In literature there is a large variety of cohesive zone laws. Most of them are categorized into the following groups: polynomial law, exponential law, trapezoidal law, bilinear law [14]. Needleman [10] in 1992 used polynomial type of cohesive laws to simulate particle de-bonding metal matrices. It is used to predict normal separation. This framework describes the interfacial decohesion process from initial debonding through complete separation. Traction-separation relation is characterised to introduce characteristic length. Tvergaard and Hutchinson [15] in 1992 proposed a trapezoidal cohesive zone model to determine crack growth resistance. They solved the problem for elasto-plastic material. Parameters involved in the traction separation law are work of separation per unit area and the peak traction. Cohesive laws can be uncoupled or coupled. Camacho and Ortiz [13] in 1996 used linear cohesive zone model to simulate multiple cracking along arbitrary paths under impact damage in brittle materials. The normal traction in an uncoupled cohesive law is independent of the tangential opening displacement and the tangential traction is independent of the normal opening displacement. Xu and Needleman [11] in 1994 proposed an exponential model to solve the problem of particle matrix decohesion. It is a coupled cohesive law and it can predict both normal and tangential separation. In coupled cohesive zone law, both tractions depend on the both normal and tangential opening displacement. When this law was investigated in mixed-mode loading, only for q=1 a physically realistic behaviour was obtained. To overcome this limitation of the Xu and Needleman law a simplified cohesive zone law was proposed by Bosch, Schreurs, and Geers [14] in 2006. It has four independent parameters and it describes mixed-mode decohesion process better.

The traction-separation relation for most of the models are such that, with an increase of interfacial separation, the traction across the interface initially increases and reaches a maximum, and then decreases and finally becomes zero showing complete material separation. There are various shapes of CZMs based on the factors which describe the shape. The different shapes of traction-separation law which can be used in the formulation of cohesive zone are shown in the Fig 1.2 [4]. Tvergaard and Hutchinson [15] in 1992 showed that the shape of cohesive zones are relatively unimportant for elasto-plastic materials.

Composite delamination has been studied by Crisfield et al.(1997) [16], Mi et al.(1998) [17] and Chen et al.(1999) [18] and they have proposed elastic-damage interface models. Geubelle and Baylor [12] in 1998 utilized bilinear cohesive zone model to study the impact of induced delamination of laminated composites. The method captures the locations of the initiation of damage, and the

various failure processes involved in the delamination event, including the critical matrix cracking and the spontaneous propagation under mixed-mode conditions of the delamination front.
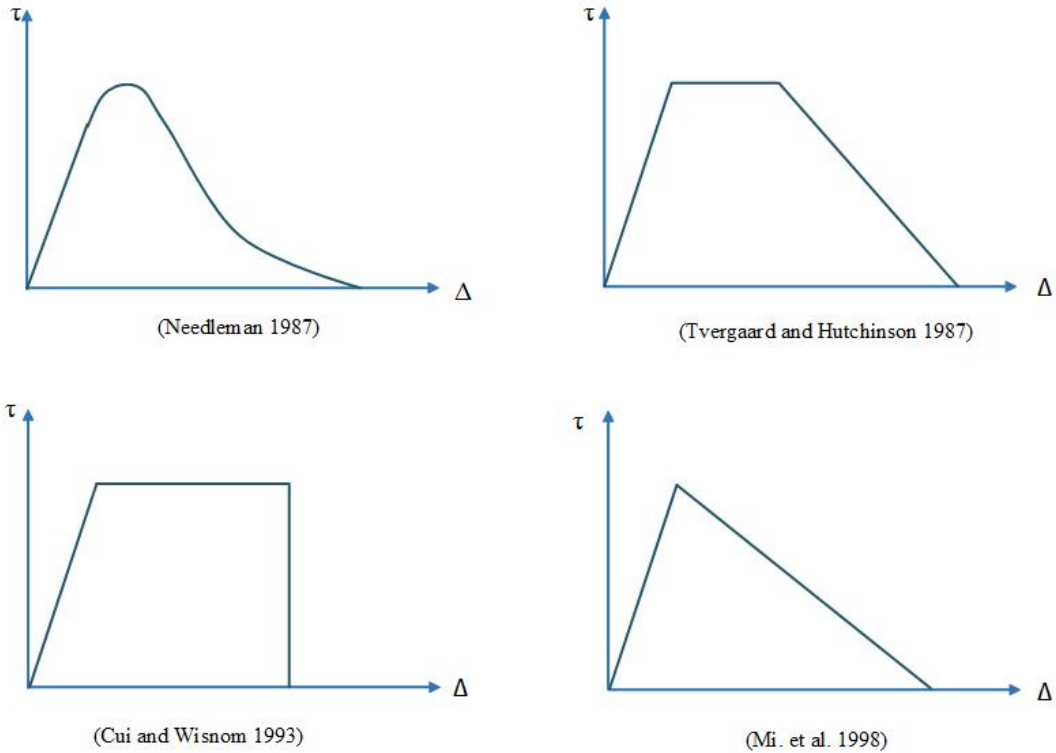
Figure 1.2: Different forms of Traction-separation laws

Adhesively bonded repairs of structures can offer substantial benefits relatively to mechanical fastening method. The most used methods to adhesively bond damaged structures consist of single or double strap, scarf and step configurations. Yang et al. [19] developed a mode-dependent embedded-process-zone (EPZ) model to simulate the mixed-mode fracture of plastically deforming adhesive joints. Jian et al. [20] used pull-off tests to characterise the debonding failure of adhesively bonded structures. These tests are conducted to validate design concept for attaching frames and bulkheads to the fuselage skin. Z. Q. Qian, A. R. Akisanya [21] in 1998 performed experiments to investigate the stress singularity near the free edge of the scarf joints. To remove stress singularity, appropriate scarf angle and material combination can be chosen. The edge failure of a scarf joint is controlled by the free edge fracture toughness. They also performed investigation of failure initiation in bonded joints [22]. The joints fail near the interface corner and crack growth occurs along the interface. Failure initiation criterion is based on small scale yielding near the interface corner. A cohesive mixed-mode bilinear model was proposed by Campilho et al. [23] for modelling single and double lap repairs on composite material. They showed that the main parameters affecting the performance of repair are specimen geometry, patch thickness and stacking sequence. In 2008, they also developed a trapezoidal cohesive mixed mode model [1] to predict the tensile behaviour of CFRP single-strap repairs. The model was studied to understand the effect of different overlap lengths and patch thickness on delamination mechanism.

4

In this work we have used the formulation developed by Turon et al. [5]. They have proposed a damage model for simulation of delamination in advanced composites under variable mode loading. Delamination initiation criteria is proposed to account for changes in loading mode in thermodynamically consistent manner. The delamination propagation criteria proposed was based on the measurement of mixed-mode fracture toughness proposed by Benzeggagh and Kenane [24]. They developed MMB (Mixed-mode bending apparatus) test to measure the mixed-mode delamination fracture toughness of unidirectional glass or epoxy composite. It allows characterisation of the delamination initiation and growth for any value of $\frac{G_{II}}{G_T}$ modal ratio. We have used this formulation to study the delamination onset and growth under static loading conditions. The finite element analysis is carried out on adhesively bonded single and double stepped CFRP laminates to investigate its mechanical behaviour.

1.3 Motivation

Composite materials are being increasingly used in many engineering applications due to their low specific weight and good mechanical properties. The presence of an interface in the composite affects its strength and stiffness; and therefore changes its fracture behaviour. It's complex material behaviour increases difficulty is designing and assessing structural repairs. Bonded repairs are cost effective, mechanically efficient and can be applied to an inspectable damage tolerant repair. Various types of bonded joints exist: overlap, scarf and stepped lap repair. Interface delamination is dominant mode of failure in stepped lap joints in CFRP materials. Scarf and stepped lap repairs are recommended when high strength recovery is required in composite structures such as astronautic and aeronautic applications. For these applications, Hart-Smith developed scarf and stepped lap joints between metal and composite adherands [25].

The interface delamination in adhesively bonded CFRP joints can be studied using experimental methods. Then based on experimental results, the analytical and numerical models are developed to model the interface delamination to reproduce experimental results. The numerical models developed can be applied to more complex structures for their analysis. Cohesive zone modelling is a promising way to simulate the interface delamination in composites under mixed mode conditions. A cohesive zone model is to be developed to estimate the damage initiation and ultimate failure under mixed-mode loading.

1.4 Objective and methodology

The objective of the thesis is to model mixed-mode delamination under static loading condition for single and double stepped lap uni-directional CFRP joint. In order to achieve the above objective, methodology used is as follows:

1. Experimental investigation of mode I and mode II fracture toughness of an adhesive layer embedded in between UD CFRP laminate using DCB and ENF specimen respectively.

2. Based on the experimental results, a traction-separation law is developed using compliance calibration method to match the load-displacement curve for test specimen.

3. Mixed mode cohesive zone modelling using two methods: (a) modified mode I cohesive crack method (proposed) (b) Benzeggagh-Kenane method.

4. Using fracture toughness obtained from experiments modelling single sided and double sided step lapped joint.

Chapter 2

Interface damage modelling

2.1 Introduction
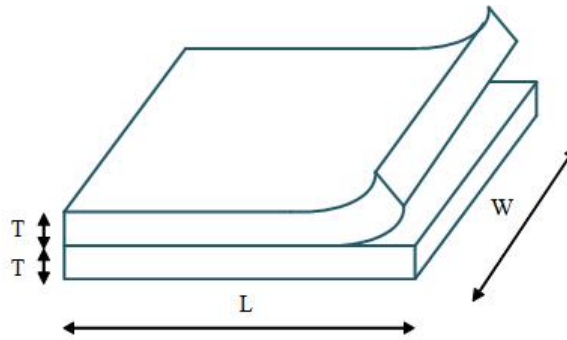
Figure 2.1: Delamination in composite

Delamination is the failure of interface between the adjacent laminae. This failure results in the separation of the laminae as shown in the Fig 2.1. While the composites have good strength in the fibres direction, they have low resistance to delamination. At microscopic level, the growth of a delamination is preceded by the formation of a damage zone ahead of the crack tip. The size and the shape of the zone depends on the material and the loading condition. The three modes of delamination are observed in composites and the schematic is shown in the Fig 2.2 [9]. They are (1) Mode I or opening mode: tensile force acts normal to the plane of crack, (2) Mode II or sliding mode: shear stress acts parallel to the plane of crack and is perpendicular to the crack front, and (3) Mode III or tearing mode, shear stress acts parallel to the crack plane and parallel to the crack front. Existence of above modes in its pure state is rarely observed and quite often we observe combination of multiple modes acting on a delamination which is defined as mode-mixity. Due to this mode-mixity delamination modelling is a challenging task.

Experimental and modelling research has examined the applicability of fracture mechanics to the problem of crack growth in composite materials. The modelling approaches for the prediction of delamination growth in laminated composites were initially based on a direct application of fracture mechanics and were performed using finite element models of the composite structure [24]. Another approach involves damage mechanics which based on the concept of cohesive zone model.
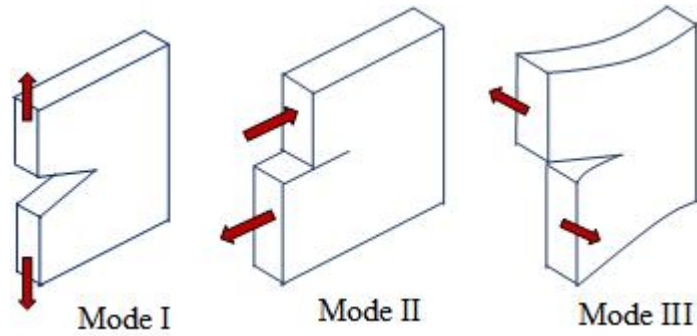
Figure 2.2: Modes of Delamination

2.1.1 Fracture mechanics approach

Fracture mechanics is a field of mechanics which studies the crack propagation in the material. The traditional fracture mechanics approach determines material failure by energy criteria in conjunction with strength criteria. Experimental work has involved measurement of the fracture mechanics parameters that characterise the resistance to delamination growth and their sensitivity to environmental conditions. It considers failure to be propagating throughout the structure. Fracture mechanics approach prominently uses two techniques: (a) Virtual crack closure technique (b) J integral. In this section subsequently these two methods are discussed at length.

Virtual crack closure technique (VCCT)
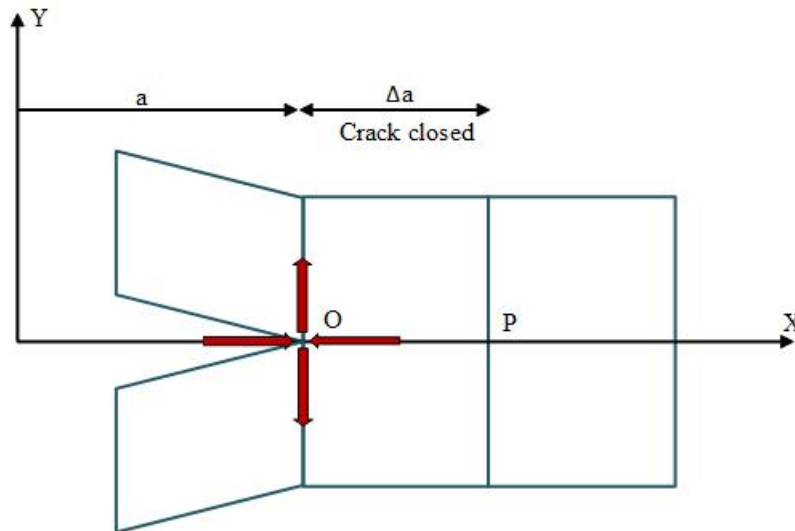
Figure 2.3: Energy release rate calculation using VCCT

It is most widely used procedures to predict crack propagation. It gives the total energy release rate as a function of the direction in which crack was extended virtually, yielding information on the most likely growth direction. This method is based on the assumption that the energy ΔE released when the crack is extended by Δa from a to $a + \Delta a$ is identical to the energy required to close the

8

crack from point p to o. It is shown in the Fig 2.3. The mode I, mode II, and mode III energy release rates, are calculated. The total energy release rate is given by,

$$G_T = G_I + G_{II} + G_{III} \tag{2.1}$$

Crack propagation is predicted when the computed energy release rate is equal to the fracture toughness of the material. The advantage of this method is that it is based on the energy and not on the stress. Limitation is that only crack propagation can be predicted. It cannot be used to predict the crack initiation.

J Integral

Linear elastic stress analysis of sharp cracks predict infinite stresses at the crack tip. In real materials stresses at the crack tip are finite because the crack tip radius must be finite. J. Rice in 1968 proposed a fracture parameter called J-integral to capture the elasto-plastic fracture behaviour [26]. The magnitude of J-integral represents the non-linear energy release rate due to crack. J-integral can be viewed as energy parameter, comparable to G and as a stress intensity parameter comparable to K.
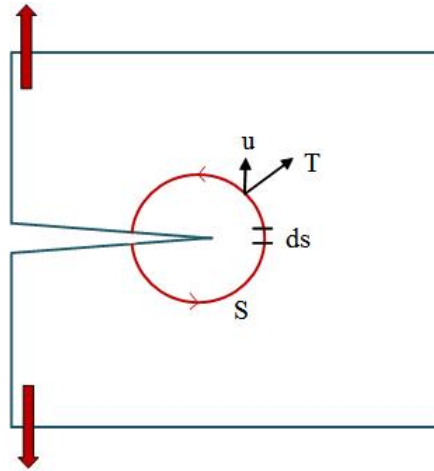
Figure 2.4: J-integral

The J-integral is carried out along an arbitrary path, which starts from the crack face and ends upon the other face, while going around the crack tip as shown in the Fig.2.4. J can be calculated as follows,

$$J = -\frac{\partial \pi}{\partial A} \tag{2.2}$$

In general, $\pi = U - F$ where, π is potential energy, U is strain energy stored, F is work done by external force and A is the crack area.

The strain energy stored in elastio-plastic material is not released when the crack grows. The crack growth in such materials leaves a plastic deformation. Thus, in elastio-plastic materials, the J value relates the difference in energy absorbed by the specimen with neighbouring crack sizes.

2.1.2 Damage mechanics approach

Damage models describe evolution of degradation phenomena from initial state up to creation of crack in the material element. It predicts initiation, propagation and fracture of materials. Damage evolution does not takes place immediately after initiation, and it requires a damage model to predict the behaviour. This approach of damage mechanics is based on the concept of cohesive crack model which is developed near the crack front. The origin of cohesive zone model can be explained on the basis of strip yield model.

Strip-yield model

The strip yield model was proposed by Dugdale and Barenblatt [9]. The model assumed a long, slender plastic zone of length ρ at the crack tip as shown in Fig 2.5. A compressive stress equal to the yield stress is applied at each crack tip. Mathematically stresses at the crack tip are infinite. To overcome this, they introduced cohesive models.
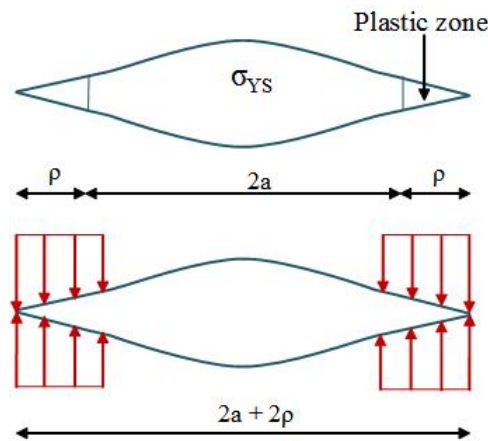
Figure 2.5: Strip yield model

The crack is divided into two parts: one part which is stress free and the other is loaded with cohesive stress. The stresses are finite in the strip yield zone and therefore there cannot be stress singularity at the crack tip. The plastic zone length must be chosen such that the stress intensity factors from the remote tension and closure compressive stress cancel one another.

Cohesive zone model

Cohesive zones project all damage mechanisms in and around a crack tip on the interface. It leads to a constitutive relation between the traction and opening displacements [14]. Damage initiation is related to the inter-facial strength. When the area under the traction-displacement jump relation is equal to the fracture toughness, the traction is reduced to zero and new crack surfaces are formed [5]. The cohesive zone model does not represent any physical material, but describes the cohesive forces which occur when material elements are being pulled apart. Cohesive zone model has advantages over conventional methods in fracture mechanics and it is able to predict the behaviour of un-cracked structures. The cohesive element is shown in the Fig 2.6.
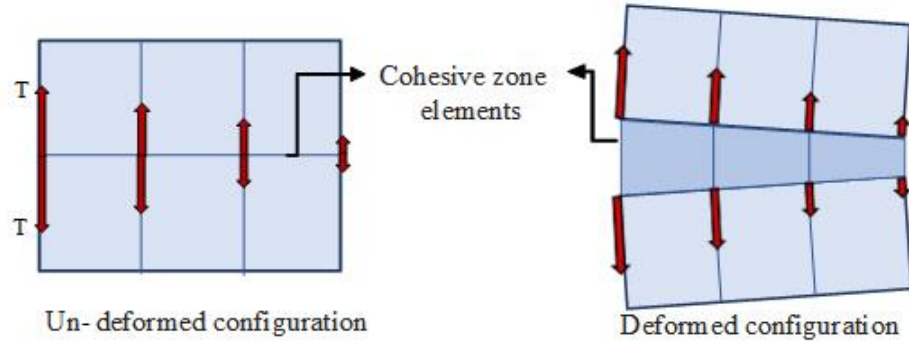
Figure 2.6: Cohesive element

The material behaviour at the interface is characterised by the stresses and the separation distances. The parameters which are required to define cohesive zone law are cohesive strength, cohesive energy, and cohesive length. Cohesive strength is the maximum resistance offered by the material to fracture. Cohesive energy is the energy dissipated when the material gets separated. Cohesive length is the separation value corresponding to the cohesive strength. The constitutive equation for cohesive zone relates the traction at the interface to the displacement jump and it can have different shapes depending on the parameters defining it. Among different cohesive zone laws, bilinear law is the simplest and it resembles closely to the actual delamination process.

2.2 Bilinear cohesive zone model for delamination

2.2.1 Mode I delamination model
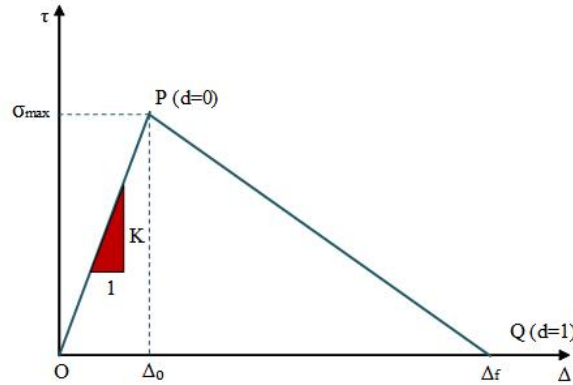
Figure 2.7: Traction-separation law for mode I bilinear model

The linear softening model defined by Guebelle [12] is a one-dimensional displacement-traction relationship. The main characteristic of bilinear cohesive zone law is high initial stiffness followed by linear softening. Fig2.7 shows the traction-separation law for bilinear model. When the maximum traction σ_{max} is reached, the interface delamination process starts. This point is termed as onset

of delamination and is represented by point P in the figure. The area under the traction-separation curve is equal to the mode I fracture toughness, G_{Ic} of the material. When the energy absorbed by the interface is equal to the fracture toughness, material fails completely and it cannot take any further load. Point Q represents the completion of the delamination.

$$T_n = \sigma_{max} \frac{D}{1-D} \frac{\Delta_n}{\delta_n} \tag{2.3}$$

where, σ_{max} is the maximum normal cohesive strength, Δ is current displacement and D is defined as $D = min(\Delta_0, max(0, 1-\Delta))$. D is the damage variable which controls complete material failure and loading-unloading conditions and When Δ is less than $(1 - \Delta_0)$, cohesive traction increases linearly with separation and it corresponds to artificial initial elastic range in the model. When Δ is greater than $(1 - \Delta_0)$, the cohesive traction is given by:

$$T_n = \sigma_{max} \frac{1-\Delta}{\Delta} \frac{\Delta_n}{\delta_n} \tag{2.4}$$

2.2.2 Mode II delamination model
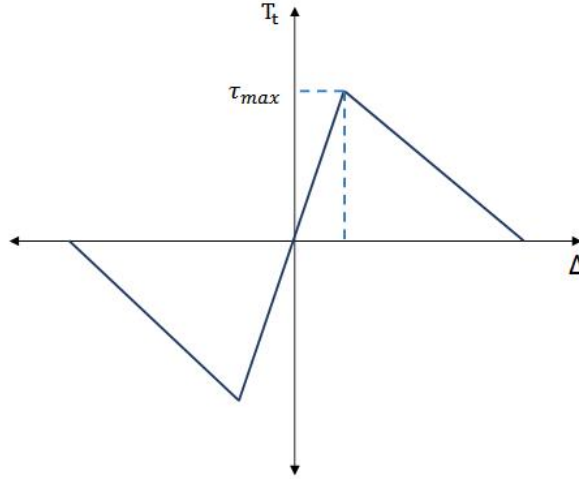
Figure 2.8: Traction-separation law for mode II bilinear model

The linear softening model developed by Guebelle [12] also defines the mode II traction-displacement relationship. Fig2.8 shows the traction-separation law for bilinear model under shear loading. Similar to the mode I definitions, bilinear model for shear loading can be defined as follows:

$$T_t = \tau_{max} \frac{D}{1-D} \frac{\Delta_t}{\delta_t} \tag{2.5}$$

Above equation is valid when Δ is less than $(1-\Delta_0)$. In the softening region, traction can be written as:

$$T_t = \tau_{max} \frac{1-\Delta}{\Delta} \frac{\Delta_t}{\delta_t} \tag{2.6}$$

2.2.3   Mixed-mode (I+II) delamination model

Boundary value problem
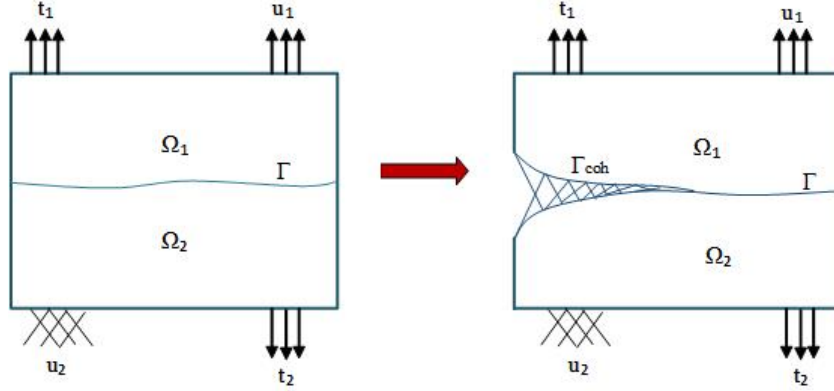
Figure 2.9: Boundary value problem

The formulation explained in this section is developed by Turon [4]. Consider a domain with a crack present in it as shown in Fig 2.9. Γ represents the crack present in the domain. Cohesive law is active on the some part of the crack denoted by Γ_{coh} and is called as fracture process zone. Consider this crack as a part of material discontinuity which will divide our domain into two parts. Equilibrium equation is: $\sigma_{ij,j} = 0$ in domain Ω as body forces are zero.

Boundary conditions are:

$\sigma_{ij}n_j = t_i$ tractions are imposed on boundary Γ_f.

$\sigma_{ij}n_j^+ = \tau_i^+ = -\tau_i^- = \sigma_{ij}n_j^-$ on the fracture process zone.

σ_{ij} is a stress tensor due to external loading. τ_i^+ and τ_i^- are closing tractions. The relation between the stress tensor and closing traction is given by the above equations.

The displacement jump across the material discontinuity can be written as

$$[|u_i|] = u_i^+ - u_i^-$$

where u_i^+ and u_i^- denotes the displacement of the points on the surface of material discontinuity. The displacement jump tensor for the interface can be written as

$$\Delta_m = \Theta_{mi}[|u_i|] \tag{2.7}$$

where Θ_{mi} is an orthogonal rotation tensor relating the local coordinate system to the global coordinate system, and Δ_m is displacement jump tensor in the local coordinate system.

Material discontinuity is modelled using a law which relates the cohesive traction to displacement jump in the local coordinates. The constitutive law is given by,

$$\tau_j = D_{ji}^{tan}(\Delta_i) \tag{2.8}$$

D_{ji}^{tan} is a constitutive tangent stiffness tensor. The constitutive model used here is proposed by Turon [4] and it is based on the free energy. Free energy is the work done in breaking the bonds

13

between a unit area of atoms. Interface free energy is the contribution to the free energy of a system due to presence of an interface. The free energy per unit surface of interface is

$$\psi(\Delta, d) = (1 - d)\psi^o(\Delta)$$

where d is scalar damage variable and ψ^o is convex function in displacement jump space. Damage variable value ranges from 0 to 1. 0 represents the onset or initial condition and 1 represents the fully damaged condition or propagation condition.

$$\psi^o(\Delta) = \frac{1}{2}\Delta_i D^o_{ij}\Delta_j$$

Interpenetration is prevented by the contact and therefore negative values of Δ_3 do not have any physical meaning. The modified free energy equation to prevent interfacial penetration can be written as

$$\psi(\Delta, d) = (1 - d)\psi^o(\Delta_i) - d\psi^o(\bar{\delta}_{3i}\langle -\Delta_3\rangle) \tag{2.9}$$

The constitutive equation for is obtained by differentiating the free energy with respect to displacement jump.

$$\tau_i = \frac{\partial \psi}{\partial \Delta_i}$$

$$\tau_i = (1 - d)D^o_{ij}\Delta_j - dD^o_{ij}\bar{\delta}_{3j}\langle -\Delta_3\rangle \tag{2.10}$$

D^o_{ij} represents the undamaged stiffness tensor and it is a function of penalty stiffness, K.

$$D^o_{ij} = \bar{\delta}_{ij}K$$

In the Voigt notation the constitutive equation can be written as

$$\tau = \left\{ \begin{array}{c} \tau_1 \\ \tau_2 \\ \tau_3 \end{array} \right\} = (1 - d)K \left\{ \begin{array}{c} \Delta_1 \\ \Delta_2 \\ \Delta_3 \end{array} \right\} - dK \left\{ \begin{array}{c} 0 \\ 0 \\ \langle -\Delta_3\rangle \end{array} \right\} \tag{2.11}$$

To evaluate the value of damage variable d at every time step of the deformation process norm of displacement jump tensor is defined.

Norm of displacement jump tensor

Delamination is a mixed-mode phenomena. To account for mode-mixity, displacement jumps in all the three modes are considered. Norm of displacement jump tensor is used to compare different stages of displacement jump state so that it is possible to define concepts as loading, unloading and reloading. The schematic representation of the norm of displacement jump tensor is shown in the Fig 2.10.

$$\lambda = \sqrt{\langle \Delta_3\rangle^2 + (\Delta_{shear})^2} \tag{2.12}$$

where Δ_3 is displacement jump in mode I and $\Delta_{shear} = \sqrt{\Delta_1^2 + \Delta_2^2}$. Δ_1 and Δ_2 are displacement
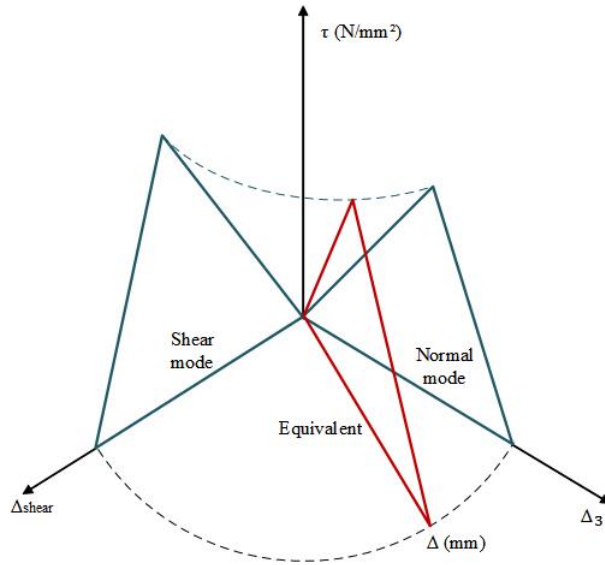
Figure 2.10: Mixed mode delamination

jumps in mode II and mode III. MacAuley's bracket is used for the mode I displacement jump to avoid interpenetration.

Damage criterion

When the load applied is pure mode I, mode II or mode III in nature, delamination starts when interlaminar traction exceeds its respective maximum interfacial strength. Under mixed mode loading interaction between modes take place. Ye's criterion [5] is used to account for the interaction.

$$\left(\frac{\langle\tau_3\rangle}{\tau_3^o}\right)^2 + \left(\frac{\tau_2}{\tau_2^o}\right)^2 + \left(\frac{\tau_1}{\tau_1^o}\right)^2 = 1 \tag{2.13}$$

Damage evolution law
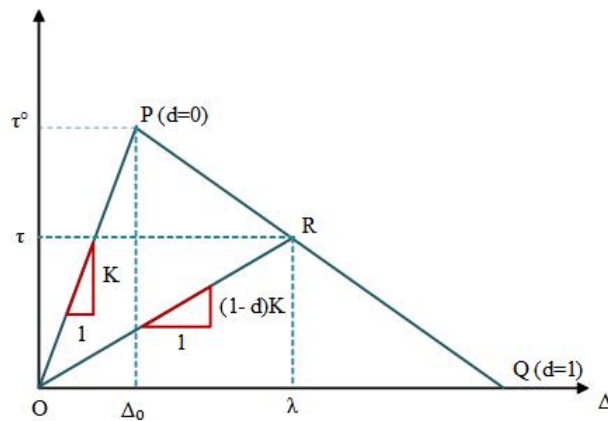
Figure 2.11: Bilinear model with damage evolution

15

The graph in the Fig 2.11 represents the damage evolution in the material. The change in the slope from K to (1-d)K represents the change in the stiffness of the material with damage evolution. The damage variable 'd' is zero at the start of the delamination(Point P) and it is equal to 1 at the completion of the delamination. If during the process, loading is stopped at point R and then unloaded, at the next loading cycle, the traction-separation law will follow O-R-Q path. This is the result of damage in the previous steps which is irreversible.

The separation value λ can be written as a function of damage variable, traction and initial stiffness of the material.

$$\lambda = \frac{\tau}{(1 - d)K}$$

Substitute the value of penalty stiffness in terms of maximum traction(τ^o) and onset displacement(Δ^o).

$$\lambda = \frac{\tau}{(1 - d)}\frac{\Delta^o}{\tau^o}$$

In order to get λ in terms of separations, tractions terms are eliminated.

$$\frac{\tau}{\tau^o} = \frac{\Delta^f - \lambda}{\Delta^f - \Delta^o}$$

Now λ can be written as

$$\lambda = \frac{\Delta^o}{(1 - d)}\frac{\Delta^f - \lambda}{\Delta^f - \Delta^o}$$

Simplify the above equation to get damage evolution law.

$$G(\lambda) = d = \frac{\Delta^f(\lambda - \Delta^o)}{\lambda(\Delta^f - \Delta^o)} \tag{2.14}$$

Damage propagation criterion

It is known that, when the energy release rate exceeds the critical energy release rate, delamination grows. Benzeggagh and Kenane [24] carried out experiments to study the delamination growth under mixed mode loading. Based on that they proposed an expression for critical energy release rate:

$$G_c = G_{Ic} + (G_{IIc} - G_{Ic})\left(\frac{G_{shear}}{G_T}\right)^\eta \tag{2.15}$$

where η is the characteristic parameter of material. The energy release rate under mixed mode loading is $G = G_I + G_{shear}$ and energy release rate for shear loading is defined as $G_{shear} = G_{II} + G_{III}$. The area under the traction-displacement jump curve is equal to the fracture toughness. Therefore,

$$G_c = \frac{1}{2}K\Delta^o\Delta^f$$

Using above two equations, propagation criteria is derived in terms of displacement jump space.

$$\Delta^f = \frac{\Delta_3^o\Delta_3^f + (\Delta_{shear}^o\Delta_{shear}^f - \Delta_3^o\Delta_3^f)\left(\frac{G_{shear}}{G_T}\right)^\eta}{\Delta^o} \tag{2.16}$$

where Δ_3^o and Δ_{shear}^o are pure mode onset displacements and Δ_3^f and Δ_{shear}^f are pure mode final displacement jumps. The mixed-mode ratio β is the ratio of displacement jumps and is given by

$$\beta = \frac{\Delta_{shear}}{\Delta_{shear} + \langle \Delta_3 \rangle} \tag{2.17}$$

The ratio $\frac{G_{shear}}{G_T}$ is defined in terms of displacement jumps as

$$B = \frac{G_{shear}}{G_T} = \frac{\beta^2}{1 + 2\beta^2 - 2\beta} \tag{2.18}$$

Based on the propagation criteria and damage evolution law, Turon et. al. [4] proposed the criteria for onset separation. This formulation assures smooth transition for all mixed-mode ratios between the initial damage surface to the propagation surface through damage evolution.

$$(\tau^o)^2 = (\tau_3^o)^2 + ((\tau_{shear}^o)^2 - (\tau_3^o)^2)B^\eta \tag{2.19}$$

Delamination initiation criterion in terms of displacement jump space can be written as

$$(\Delta^o)^2 = (\Delta_3^o)^2 + ((\Delta_{shear}^o)^2 - (\Delta_3^o)^2)B^\eta \tag{2.20}$$

This formulation takes into account the mixed mode ratios and therefore is applicable to in general static loading conditions.

Chapter 3

Experimental characterisation of interface properties

3.1 Introduction to fracture toughness

Experimental work involves the measurement of fracture mechanics parameters that characterise the resistance to delamination growth. These material properties are used as input for FEA. In the present work, the fracture toughness (mode I and mode II) of unidirectional CFRP are measured which are then used in cohesive zone modelling. Mode I and Mode II fracture toughness tests, double cantilever beam (DCB) and end notched flexure (ENF) tests are respectively conducted on the CFRP laminate. Also, mixed mode bending (MMB) test is carried out the to get the fracture toughness for a combination of various mode I and mode II loadings. Fracture toughness is an important factor for CZM. The area under the traction-separation curve is the energy required for crack propagation and it is equivalent to fracture toughness. Other parameters of CZM can be derived from fracture toughness, and they are used to model debonding and delamination.

3.1.1 Standard test methods

Delamination in the laminated composites affect their structural performance. The inter-laminar performance of a composite is identified by weakness under both normal and shear stresses. The delamination and its growth is described by strain energy release rate and the manner in which load is applied. A delamination may be loaded in mode I(opening), mode II(sliding), mode III(tearing), or may be in the combination of these modes. The critical strain energy release rate varies with the mode of loading. To characterise the delamination resistance for different loading conditions various test methods are developed. The ASTM standard, ASTM D 5528 [27] describes the use of double cantilever beam(DCB) specimen to determine the mode I fracture toughness G_{IC} of fibre reinforced polymer composites under mode I tensile loading. To study delamination failure under mode II End notch flexure(ENF) and End loaded split(ELS) test are used. The ASTM standard, ASTM D 7905 [28] recommends the use of end notch flexure(ENF) test to measure the mode II fracture toughness G_{IIC} of fibre reinforced polymer composite laminates under mode II shear loading. ASTM D 6671 [29] explains the use of mixed mode bending(MMB) test to detect the inter-laminar fracture

toughness of fibre reinforced composite materials over a wide range of combinations of various mode I and mode II loading. The specimen preparation involves two types of methods. One method includes the use of adhesive to bond the two adherands and other method includes the use of aluminium foil to create a crack in the laminate.

3.2 Fracture toughness of adhesive layer in CFRP

During service, various damages occur in the CFRP panels. The damage in the composite reduces the strength of the structures which is associated to the recycling difficulties and replacement costs [1]. To restore the functioning of component, it is more efficient to repair the structures than replacing them [23]. The repair of structure with composite patch can be carried out in two ways: i) Mechanical fastening or ii) adhesive bonding. Mechanical fastening method includes the use of connectors such as rivets, bolts and nuts. The main disadvantage with their use is that they result in high stress concentration and galvanic corrosion. This can be avoided by using adhesively bonded repairs and the benefits associated with it are improved appearance, good sealing properties, high strength to weight ratio and reduced stress concentration [1, 22]. Adhesively bonded repairs of structures can offer substantial benefits relatively to mechanical fastening method. The most used methods to adhesively bond damaged structures consist of single or double strap, scarf and step configurations. To characterise the debonding failure of adhesively bonded structures experimental tests are carried out.

3.3 DCB test - mode I fracture toughness of adhesive layer

The test method deals with the determination of mode I inter-laminar fracture toughness of carbon epoxy composite material using the double cantilever beam (DCB) specimen. Another aspect of the test is to determine the cohesive law that can accurately characterise the fracture behaviour. The test procedure is followed as given in ASTM D5528 [27].

3.3.1 Specimen preparation
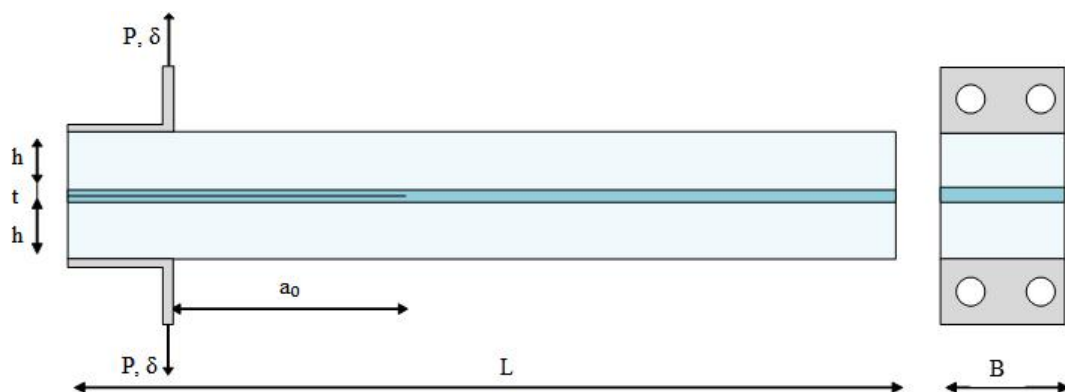
Figure 3.1: Schematic representation of DCB specimen with adhesive bonding

The CFRP laminates are prepared from unidirectional carbon fibre mat of 200 gsm weight through vacuum bagging procedure. The matrix is composed of epoxy resin CY 200 and hardener HY 951 in proportion of 10:1 by weight according to the ASTM D5528 standard [27]. The laminate is made up of 8 unidirectional layers. The carbon fibre fabric layers were stacked in the 0° direction. The mechanical properties of CFRP composite laminate are given in the Table 3.1. A ductile epoxy adhesive is used to bond the adherends at room temperature. Araldite 2015 is used as a adhesive and a constant thickness, t of $0.2mm$ was ensured. The dimensions of the DCB specimen are given in the Table 3.2. After cutting the specimens as per the given dimensions from the laminates, hinges are bonded on the top and bottom surfaces of the end of DCB specimen arm. With the help of razor blade initial crack is introduced in the specimen such that initial delamination length of 50 mm was obtained. The schematic of DCB specimen in as shown in Fig 3.1. Random speckle pattern is created on thickness side of the specimen to measure displacements through DIC.

Table 3.1: CFRP composite laminate properties

Material property	Value
Longitudinal modulus, E_{11} (GPa)	82.56
Transverse modulus, $E_{22} = E_{33}$ (GPa)	4.98
In-plane shear modulus, $G_{12} = G_{13}$ (GPa)	3.30
Out-of-plane shear modulus, G_{23} (GPa)	2.47
In-plane Poisson's ratio, $\nu_{12} = \nu_{13}$	0.31
Out-of-plane Poisson's ratio, ν_{23}	0.43

Table 3.2: Dimensions of DCB specimen

Dimension	Value
Length (L)	130 mm
Width (B)	25 mm
Thickness (h)	2 mm
Initial delamination length (a_o)	50 mm
Thickness of adhesive layer (t)	0.2 mm

3.3.2 Experimental setup

Experimental setup for the DCB test is shown in the Fig 3.2. The experiment is performed on 10kN Instron machine. 2D-DIC system is used to track the through the thickness full displacement and strain field. It has single Grasshopper CCD camera coupled with Schneider Xenoplan lenses. It is mounted on tripod and aligned with the specimen so that it can capture the images accurately. Two white light LED sources are used on both the sides of camera to ensure the proper illumination of the specimen. Aperture of the lens is adjusted to get fine field view. Camera is connected to the laptop with pre-installed image capturing software. The images on the surface of an object, before and after delamination are recorded, digitized and stored in a computer as digital images with the help of this software. First image is taken at zero load and called as reference image. In DIC post-processing, all the displacement and strain calculations are carried out with respect to this image. The tensile load is applied on the specimen through the hinges in displacement control mode. The load is applied at the rate of 2.5 mm/min as suggested in ASTM D5528. Load-displacement data is
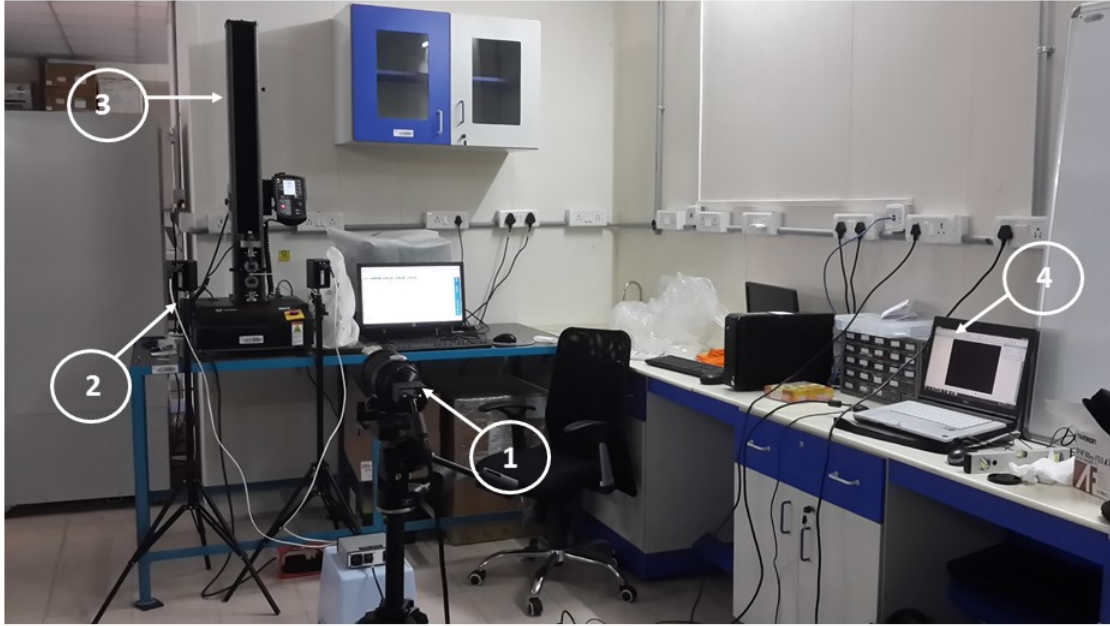
1. CCD Camera
2. LED Light source
3. Instron machine
4. PC with image capturing software

Figure 3.2: Experimental setup for DCB test

recorded continuously. Total 3 specimen are tested and the experimental image of DCB specimen is as shown in Fig 3.3.
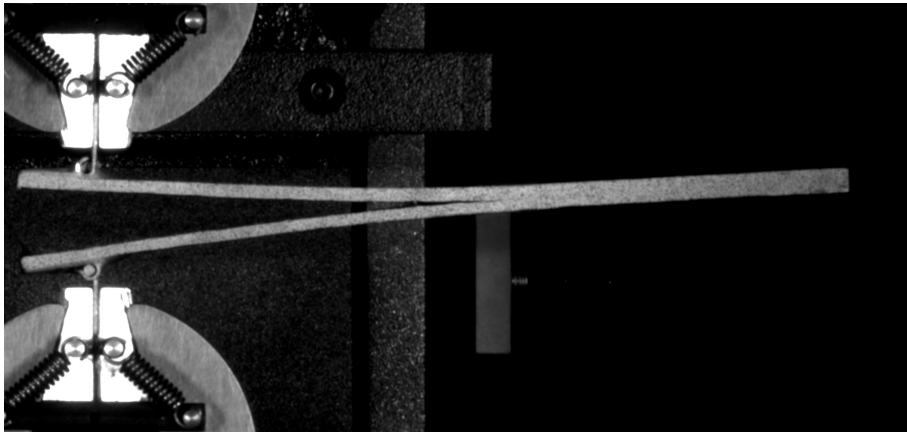
Figure 3.3: Experimental image of DCB specimen

3.3.3 Results and discussion

Digital image correlation with Ncorr

Experimental method of material characterisation depends on the surface displacement field measurement. Digital image correlation technique compares undeformed images and deformed images to get the deformation of the surface. The surface of the specimen is observed using CCD camera with

an imaging lens. The images of the surface before and after deformation, are captured, digitized and then recorded in the computer. These images are compared to detect displacements by searching a matched point from one image to other. This matching process uses area with a multiple matching points.

An open source 2D DIC software, Ncorr was used to perform DIC analysis. Ncorr provides a correspondence between points in the undeformed reference image and deformed current images. It is achieved by comparing the position of subsets in reference and current images. After getting the images, DIC is performed which includes following steps:

1. Set reference image.

2. Set current images: This includes the images on which DIC is to be performed.

3. Set region of interest(ROI): It describe the region of the image where deformation occurs.

4. Set DIC parameters.

5. DIC analysis: The seed points are used as a starting point for the calculation of displacement.

6. Format displacements and calculate strains: It is done by removing noisy displacement data by setting the cut-off.

The ncorr settings for the analysis are given in the Table 3.3 and its is used for extraction of near crack tip displacement field.

Table 3.3: Ncorr settings for DIC

Parameters	Value
Solver type	Inverse compositional Gauss-Newton solver
Subset radius	25
Subset spacing	5
Diffnorm cutoff	1e-6
Iteration cutoff	50
Number of seeds	2
Correlation coefficient cut-off	1.9984
Strain radius	15
Step analysis	Disabled

Estimation of effective delamination length using SIF estimator

Modified form of least square algorithm is used for estimation of mixed-mode SIF and calculation of crack tip location from the whole field displacement field [30].

Two-dimensional displacement field equations for the general mixed mode crack tip displacement field are given by Atluri and Kobayashi.

$$
\begin{aligned}
u_x = &\sum_{n=1}^{\infty} \frac{A_{In}}{2G} r^{n/2} \left[k cos \frac{n}{2}\theta - \frac{n}{2} cos \left(\frac{n}{2} - 2 \right) \theta + \left(\frac{n}{2} + (-1)^n \right) cos \frac{n}{2}\theta \right] \\
&- \sum_{n=1}^{\infty} \frac{A_{IIn}}{2G} r^{n/2} \left[k sin \frac{n}{2}\theta - \frac{n}{2} sin \left(\frac{n}{2} - 2 \right) \theta + \left(\frac{n}{2} - (-1)^n \right) sin \frac{n}{2}\theta \right]
\end{aligned}
\tag{3.1}
$$

$$u_y = \sum_{n=1}^{\infty} \frac{A_{In}}{2G} r^{n/2} \left[k\sin\frac{n}{2}\theta + \frac{n}{2}\sin\left(\frac{n}{2} - 2\right)\theta - \left(\frac{n}{2} + (-1)^n\right)\sin\frac{n}{2}\theta \right]$$
$$- \sum_{n=1}^{\infty} \frac{A_{IIn}}{2G} r^{n/2} \left[-k\cos\frac{n}{2}\theta - \frac{n}{2}\cos\left(\frac{n}{2} - 2\right)\theta + \left(\frac{n}{2} - (-1)^n\right)\cos\frac{n}{2}\theta \right]$$

(3.2)

where u_x is displacement along x direction and u_y along y direction, r and θ are polar coordinates of data points with respect to crack tip, n is number of parameters and G is shear modulus. Consider x_c and y_c as a location of crack tip relative to the arbitrary cartesian coordinate frame. The crack tip location is related to r and θ as:

$$r = \sqrt{(x - x_c)^2 + (y - y_c)^2}$$

$$\theta = tan^{-1}\left(\frac{y - y_c}{x - x_C}\right)$$

After considering rigid body motion for a single point p and n parameters, above equations can be written in matrix form as

$$\left\{ \begin{array}{c} u_{xp} \\ u_{yp} \end{array} \right\} = \begin{bmatrix} f_{I1}(r_p, \theta_p) & g_{I1}(r_p, \theta_p) \\ \vdots & \vdots \\ f_{In}(r_p, \theta_p) & g_{In}(r_p, \theta_p) \\ -f_{II1}(r_p, \theta_p) & -g_{II1}(r_p, \theta_p) \\ \vdots & \vdots \\ -f_{IIn}(r_p, \theta_p) & -g_{IIn}(r_p, \theta_p) \\ 1 & 0 \\ 0 & 1 \\ x_p & y_p \\ -y_p & x_p \end{bmatrix}^T \left\{ \begin{array}{c} A_{I1} \\ \vdots \\ A_{In} \\ A_{II1} \\ \vdots \\ A_{IIn} \\ T_x \\ T_y \\ cos(R) - 1 \\ sin(R) \end{array} \right\}$$

(3.3)

where T_x and T_y are rigid body translations in x and y directions and R is the rigid body rotation. f_I, g_I, f_{II} and g_{II} are trigonometric functions of polar coordinates. In a compact form we can write,

$$u_p = Q_p^T a$$

For a set of m collected data points surrounding crack tip, the assembled set of matrices for n parameter solution can be written as

$$u = C(x_c, y_c)a$$

(3.4)

where u is the vector of displacements obtained from experimental data, C is a rectangular matrix dependent on crack tip location and a is vector consisting unknown mode I and II parameters along with translation and rotation terms. The values of x_c, y_c and a are obtained by minimizing following objective function:

$$J(x_c, y_c, a) = \frac{1}{2}(u - C(x_c, y_c)a)^T(u - C(x_c, y_c)a)$$

(3.5)

For every known x_c and y_c, the objective function becomes quadratic in parameters and the closed form solution exists for the unknown parameters (a) at which the objective function attains a global minimum.

$$a = (C^T C)^{-1} C^T u \tag{3.6}$$

Select the multiple locations around the crack tip and calculate unknown parameters 'a' for each location. For every location, calculate J. Out of all the grid points as shown in Fig 3.4, select the crack tip location and unknown parameters corresponding to the location at which J attains lowest value.
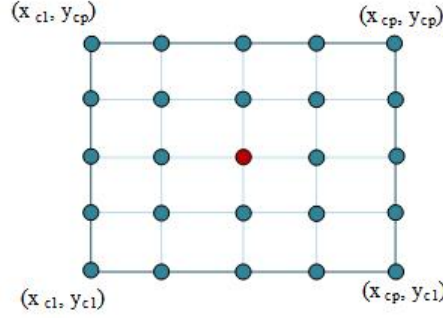
Figure 3.4: Schematic diagram of square grid used to get optimal crack tip location

In the Fig 3.4, x_{c1} and x_{cp} are the minimum and maximum x-coordinate values and y_{c1} and y_{cp} are the minimum and maximum y-coordinate values.

SIF estimation module is used for automated data collection and processing. Steps involved in the estimation of SIF are given below:

1. Specify material properties: Define the elastic modulus and poison's ratio for the material.

2. Load DIC data: DIC data from Ncorr 2D DIC software is taken as input. Input file should be .mat format.

3. Load calibration image: Load the calibration image in the GUI and select two points for distance calibration. Enter the distance between them in mm.

4. Crack tip selection: Crack tip can be selected using the graphical user interface (GUI).

5. Data collection: Data is collected from an annular region surrounding crack tip. Annular region is defined by starting and limiting radius in the graphical user interface. Starting radius: 1.5, Limit radius: 2, Step size:0.1

6. Crack tip search parameter: A square with 0.2 mm side length and 0.02 mm grid size is used to get the crack tip.

7. Solution parameter: 7 parameters are recommended for SIF estimation. Now calculate the SIF.

Result obtained from SIF Estimator is given in the Table 3.4.

Table 3.4: SIF Estimator result

Parameter	Value
Mode I SIF	9065.032
Recalculated crack tip x coordinate	58.37 mm
Recalculated crack tip y coordinate	81.50 mm
Number of parameters used for solution	7
Convergence error	0.0318

Mode I fracture toughness calculation

From experimental load versus displacement curve it can be observed that, after reaching maximum load value delamination starts and therefore load curve starts dropping. The interlaminar fracture toughness can be evaluated by three methods as mentioned in ASTM D5528 [27]. They are i) Modified beam theory (MBT), ii) Compliance calibration (CC) method, iii) Modified compliance calibration (MCC) method. In this study, compliance beam theory is used. The method is suggested by Moura [31] and uses equivalent crack length.
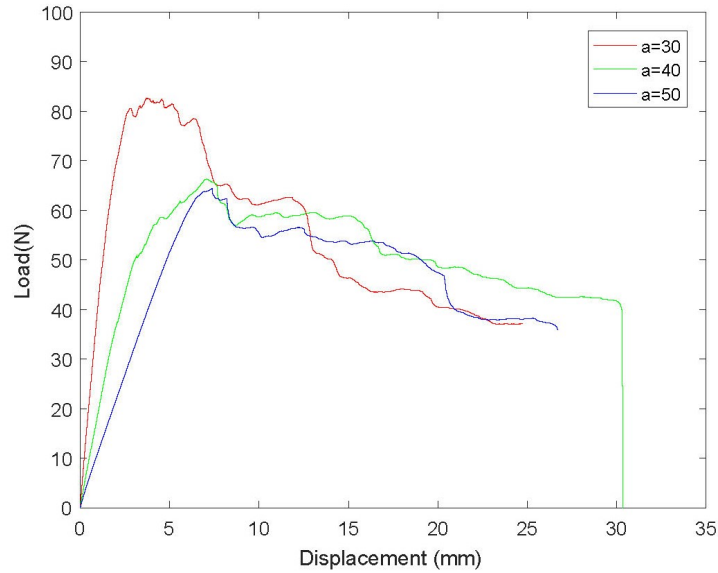
Figure 3.5: Experimental load vs displacement curve for DCB specimen

The experiments are performed at 3 crack lengths: 30 mm, 40 mm and 50 mm. The load-displacement curves for the three delamination lengths is shown in the Fig3.5. To get the correction length generate the least square plot of the cube root of compliance as a function of delamination length. Crack length correction corresponds to the intercept of the line fitted to the 3 data points as shown in the Fig3.6. The equation is:

$$y = 0.0094x + 0.0746$$

Δ is found out to be 7.936 mm. Considering crack length correction, equivalent crack length is estimated which is used for mode I fracture toughness calculation.

In this study, compliance beam theory with equivalent crack is used to get the fracture toughness.

25
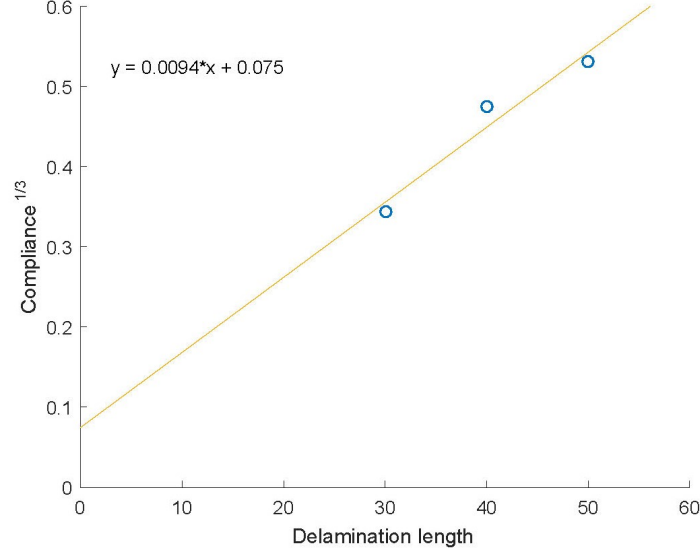
Figure 3.6: $Compliance^{1/3}$ vs a curve for DCB specimen

In this method, the crack tip opening displacement(CTOD) is expressed as a function of the strain energy release rate. The cohesive is obtained by differentiating the relationship with respect to CTOD.

$$G_I = \int_0^w (\sigma)dw \tag{3.7}$$

Differentiate the above equation

$$\sigma(w) = \frac{dG_I}{dw} \tag{3.8}$$

Using Timoshenko beam theory, the specimen compliance can be written as

$$C = \frac{8a^3}{E_1 Bh^3} + \frac{12a}{5BhG_{13}} \tag{3.9}$$

where E_1 and G_{13} are the elastic properties of the specimen arm. Consider initial crack length as a_0 and initial compliance as C_0. The equivalent flexural modulus can be obtained as

$$E_f = \left(C_0 - \frac{12(a_0 + h\Delta)}{5BhG_{13}} \right)^{-1} \frac{8(a_0 + h\Delta)^3}{Bh^3} \tag{3.10}$$

where Δ is crack length correction.
R curve i.e. the evolution of strain energy release rate as a function of the equivalent crack length can be obtained by

$$G_I = \frac{P^2}{2B} \frac{dC}{da}$$

$$G_I = \frac{6P^2}{B^2 h} \left(\frac{2a_e^2}{E_f h^2} + \frac{1}{5G_{13}} \right) \tag{3.11}$$

26

The equivalent crack method discussed above is used to obtain the R-curves. Energy release rate for mode I for all the specimen is calculated.
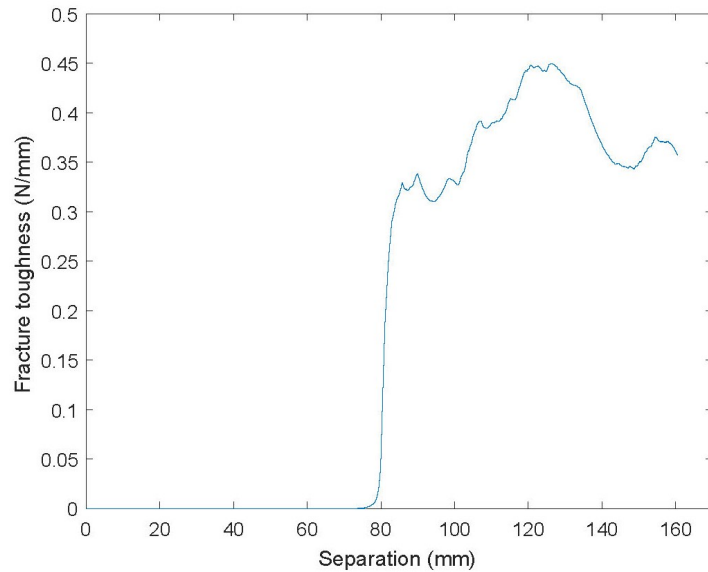
Figure 3.7: R curve for DCB specimen with adhesive layer

The equivalent crack method is used to get the R-curve for a specimen as shown in the Fig3.7. In the images obtained from DIC, the location of initial crack tip was identified. The pair of points to calculate CTOD was selected on left and right side of the crack tip location. To extract the cohesive law from the experiments, plot the curve fracture toughness vs crack tip opening displacement.
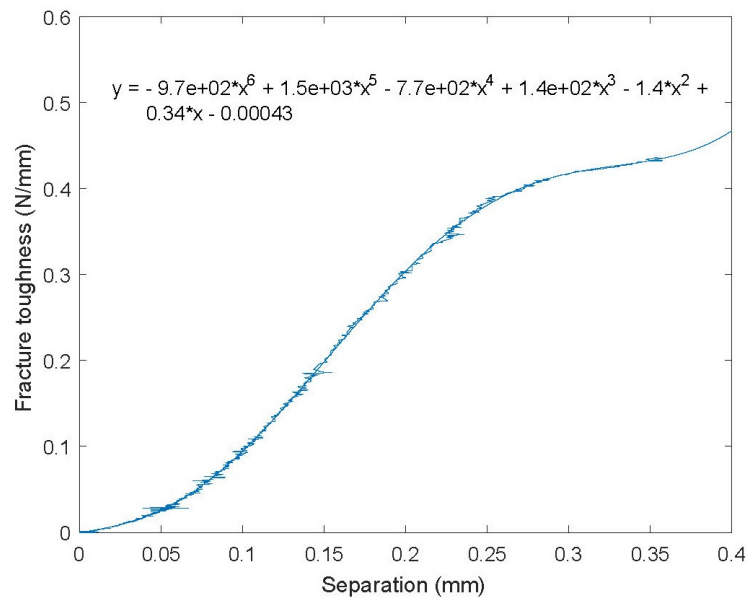
Figure 3.8: G-CTOD relation for DCB specimen with adhesive layer

After that, fit the six degree polynomial to the curve as shown in the Fig 3.8. The equation is:

$$y = -970.01x^6 + 1501x^5 - 768.72x^4 + 138.1x^3 - 1.399x^2 + 0.3381x - 0.0004$$

Differentiate the with respect to CTOD to get the relation between traction and crack tip opening displacement. Plot the traction equation against CTOD. That will give the traction-separation law for the given case as shown in the Fig 3.9.
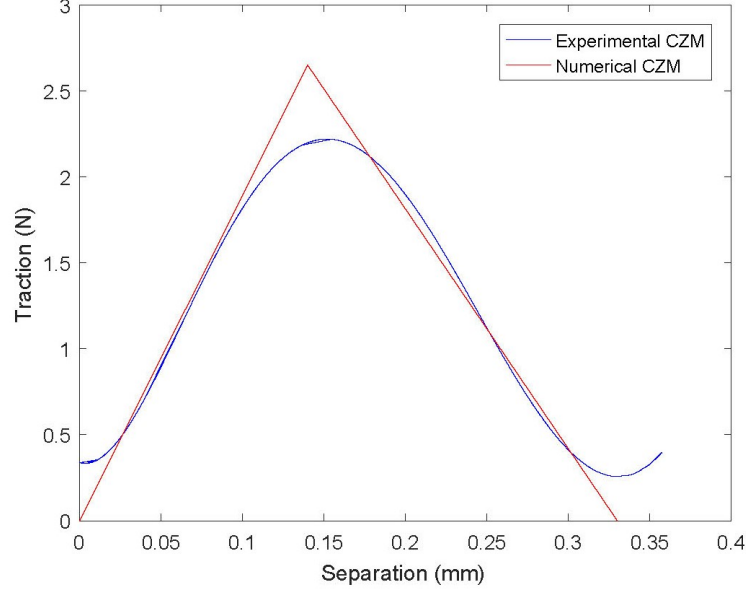
Figure 3.9: Mode I cohesive law for adhesively bonded CFRP

The mode I fracture parameters for the adhesive are given in the Table 3.5 as obtained through the experiment.

Table 3.5: Cohesive law parameters obtained from experiment: Mode I

Parameter	Value
Mode I fracture toughness	0.44 N/mm
Maximum normal traction	2.75 N
Normal separation	0.32 mm

The onset displacement is obtained as 0.17 mm. The stiffness of the material comes out to be 16.176 N/mm. Due to low stiffness value the disturbance is observed in the load-displacement curve.

Turon [4] has established a procedure to determine the optimal CZM parameters for delamination. The initial stiffness of the bilinear law is defined by transverse young's modulus, thickness of laminate and scalar parameter controlling overall stiffness in transverse direction. The initial stiffness should be high so that it will not affect overall elastic properties of composite.

$$K = \frac{\alpha E_3}{t} \tag{3.12}$$

After matching the whole field displacement for experiment and numerical method, the stiffness is found out to be 1000. The length of a cohesive zone is defined as the distance from the crack tip

28

where maximum traction is observed [4]. The length of cohesive zone can be calculated as:

$$l_{cz} = ME_3 \frac{G_c}{(\tau^o)^2} \tag{3.13}$$

where, M is a parameter corresponding to the shape of the cohesive zone model. The length of the cohesive zone comes out to be 3.185 mm. In order to obtain accurate FEM result using CZM there should be enough number of elements present in the cohesive zone. When cohesive zone is represented by too few elements, the distribution of traction ahead of crack tip is not represented clearly. It is recommended to include 5 elements in the cohesive zone [4]. The length of cohesive element in the delamination direction is recommended as 0.637 mm. The mode I fracture parameters for CFRP are given in the Table 3.6 as obtained through the experiment and the traction-separation law is shown in the Fig 3.10.
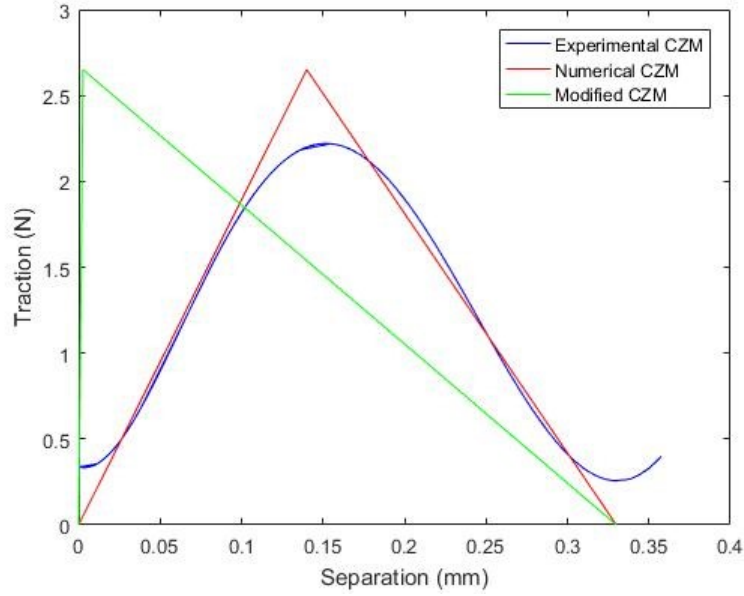
Figure 3.10: Modified mode I cohesive law for adhesively bonded CFRP

Table 3.6: Mode I cohesive law parameters for Araldite 2015

Parameter	Value
Mode I fracture toughness	0.44 N/mm
Maximum normal traction	2.75 N
Penalty stiffness	1000
Onset displacement	0.00275 mm
Normal separation	0.32 mm

3.4 ENF test - mode II fracture toughness of adhesive layer

This test method deals with the determination of the mode II inter-laminar fracture toughness, G_{IIC} of carbon epoxy composite material under mode II shear loading using the end-notched flexure

test. Six types of specimen are available for mode II fracture toughness testing. These are end notched flexure(ENF) specimen, stabilized end notched flexure(SENF) specimen, four point bend end notched flexure(4ENF) specimen, end load split(ELS) specimen, over notched flexure(ONF) specimen, and the tapered end-notched flexure specimen. Among these methods ENF test is widely used as recommended by ASTM D 7905.

3.4.1 Specimen preparation
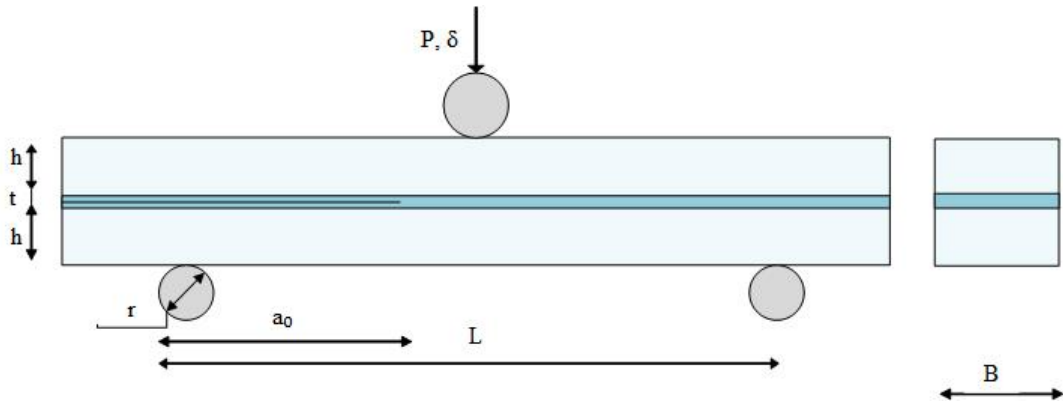
Figure 3.11: Schematic representation of ENF specimen with adhesive bonding

The method used in ENF specimen preparation is same as the method used for DCB specimen preparation. The schematic of ENF specimen is as shown in the Fig 3.11. The dimensions for the ENF specimen are given in the Table 3.7.

Table 3.7: Dimensions of ENF specimen

Dimension	Value
Overall length	130 mm
Length (L)	100 mm
Width (B)	25 mm
Thickness (h)	2 mm
Initial delamination length (a_o)	30 mm
Adhesive thickness (h)	0.2 mm

3.4.2 Experimental setup

Experimental setup for the ENF test is shown in the Fig3.12. The experiment is performed on 100kN MTS universal testing machine. Three point bending loading condition is used to perform the test. Support rollers are kept 100 mm away and loading roller is centred between the two. Loading of the specimen is performed in displacement control mode at the rate of 0.5 mm/min as given in ASTM D7905 [28]. The experiment is performed in two stages which are precracked and non-precracked. To calculate the fracture toughness in mode II, compliance calibration is carried out. First non-precrack test is performed. The specimen is fixed to get the the delamination length of 20 mm away from one of the support rollers and then load is applied. The load-displacement data for the test is recorded. This same test is performed with delamination length of 40 mm. After that specimen is arranged
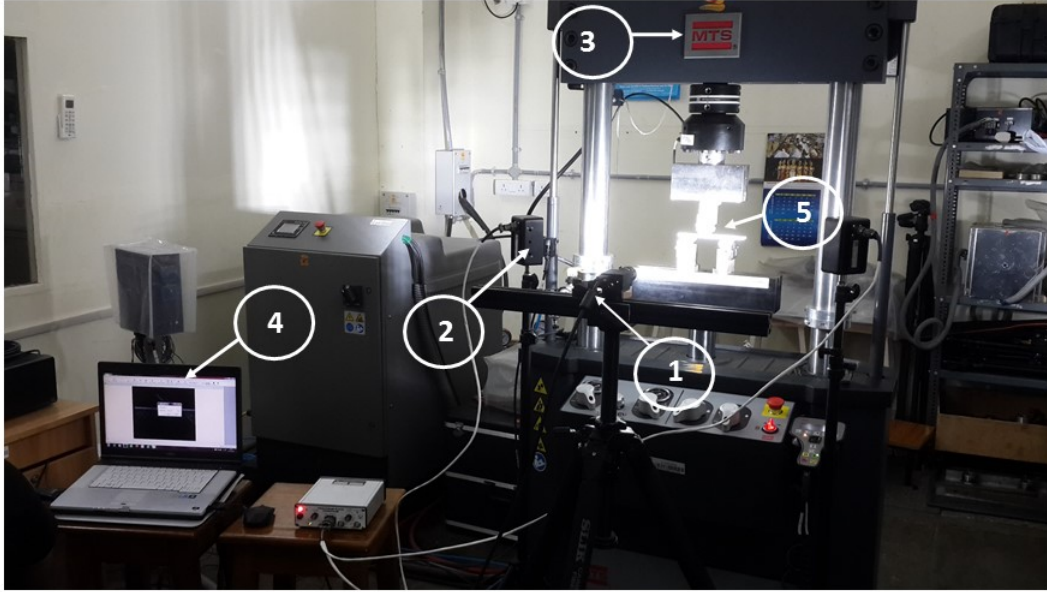
1. CCD Camera   2. LED Light source
3. MTS universal test machine   4. PC with image capturing software
5. Specimen with 3-point bend setup

Figure 3.12: Experimental setup for ENF test

to get the delamination length of 30 mm. Load is applied on the specimen till delamination starts to grow. With delamination propagation, reduction in load is observed. The new position of the delamination front is marked and non-precracked fracture toughness is calculated from extracted data. In the second stage, precracked test is performed with the same procedure followed in the first stage.

3.4.3 Results and discussion

Mode II fracture toughness calculation

The experimental load vs displacement curve for the three tested specimens is shown in the Fig3.13. From the curve it can be observed that, after reaching maximum load value delamination starts and load starts dropping. The interlaminar mode II fracture toughness can be calculated by using compliance calibration (CC) method as mentioned in ASTM D7905[28]. From load-displacement curve compliance of the specimen can be found out. G_{IIc} will be the minimum of the values calculated from PC and NPC tests. From load-displacement curve, stiffness of the specimen can be found out. Compliance is a reciprocal of stiffness.

Plot the graph of compliance vs cube of delamination length. Compliance in ENF is directly proportional to the cube of delamination length as shown in Fig3.14. Fit the curve for the equation below:

$$C = A + ma^3$$

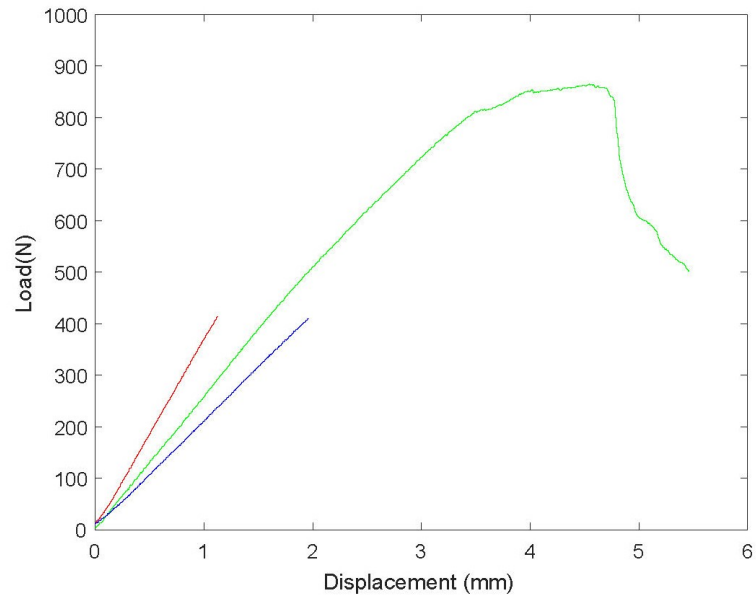A and m are compliance calibration coefficients. The value of compliance calibration coefficient are

Figure 3.13: Load-displacement curves for adhesively bonded ENF specimen

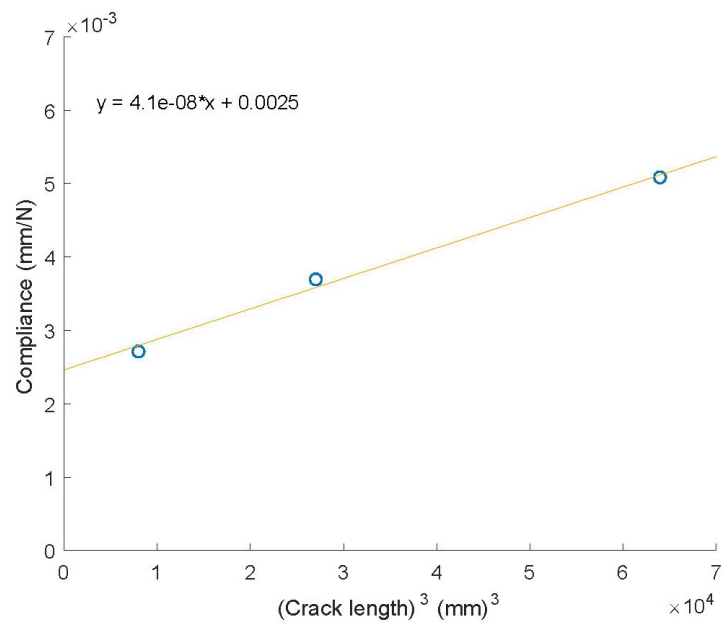obtained as A = 0.0025 and m = 4×10^{-8}.

Figure 3.14: Compliance vs a^3 curve for adhesively bonded ENF specimen

The fracture toughness can be calculated as

$$G_{IIc} = \frac{3mP_{max}^2 a^2}{2B} \tag{3.14}$$

Mode II fracture toughness for all specimen is calculated using the above equation. The result is given in the Table 3.8.

Table 3.8: Mode II fracture toughness

Specimen	1	2	3	Average
G_{II}	2.96	2.59	2.73	2.76

Numerical analysis

The ENF specimen with the given dimensions is modelled in the ANSYS15. The number of simulations are performed to get the match between experimental and numerical load-displacement curve. The mode II fracture parameters for adhesive are given in the Table3.9 as obtained through the experiment. The maximum tangential traction is assumed to be equal to the shear strength of the material and from that displacement jump is evaluated.

Table 3.9: Mode II cohesive law parameters for Araldite 2015

Parameter	Value
Mode II fracture toughness	2.76 N/mm
Maximum shear traction	25 N
Shear separation	0.1104 mm

3.5 MMB test - mixed mode (I+II) fracture toughness of adhesive layer

This test method deals with the determination of interlaminar fracture toughness, G_c of carbon epoxy composite material at various mode I to mode II loading ratios using the mixed mode bending test. There are various types of specimen available for mixed mode (I+II) fracture toughness testing. These are asymmetrical load double cantilever beam(ALDCB) test, cantilever beam opening notch(CBON) test, imposed displacement cantilever beam(IDCB) test, mixed mode flexure(MMF) test, and mixed mode bending(MMB) test. Among these methods MMB test is used as recommended by ASTM D6671.

The MMB test designed by Benzeggagh and Kenane [24] is used to get the material characteristic parameter. The method involves the characterisation of delamination initiation and growth on the basis of a strain energy release concept. Experiments are to be performed at various mode ratios including mode I and II. Total fracture toughness is plotted against modal ratio to get the material parameter. Due to lack of facilities and shortage of time we could not perform this test. The material parameter characterisation is carried out using numerical method.

3.5.1 Material parameter calibration

The study deals with the characterisation of delamination initiation and growth on the basis of a strain release rate concept. To consider for mode-mixity and to predict G_{Tc} as a function of G_{II}/G_T

modal ratio, the relationship suggested by Benzeggagh and Kenane[24] is used.

$$G_{Tc} = G_{Ic} + (G_{IIc} - G_{Ic}) \left(\frac{G_{II}}{G_T} \right)^{\eta} \tag{3.15}$$

where, G_{Tc} is a total critical fracture toughness, G_{Ic} is mode I fracture toughness, G_{IIc} is mode II fracture toughness, η is a characteristic parameter of material. Various simulations are performed by varying η. The load-displacement curves obtained with various η values is shown in the Fig 3.15. From that we observe, the best match between the experimental curve and numerical curve is obtained for the value $\eta = 3$.
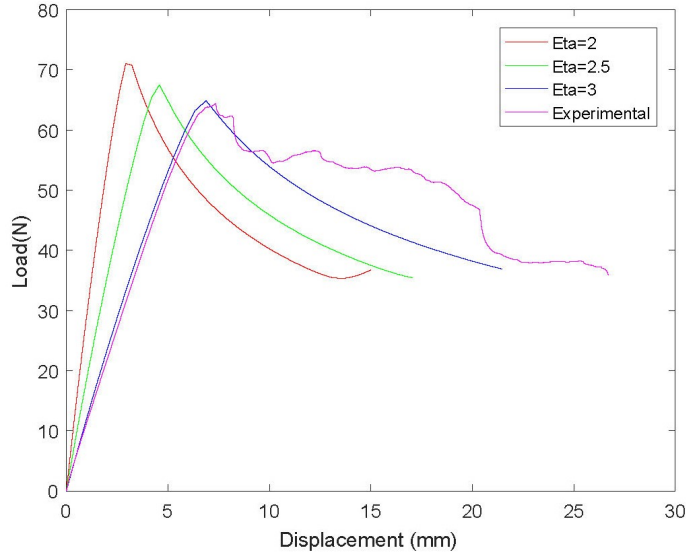
Figure 3.15: Load-displacement curves for DCB specimen varying η values

3.6 Fracture toughness of CFRP

The procedure used for fracture toughness characterisation of CFRP is same as followed in the previous section. For mode I characterisation DCB test is performed, for mode II ENF test is used. As delamination is a mixed-mode phenomena, MMB test is performed for characterisation of inter-laminar fracture toughness of CFRP at various mode I to mode II loading ratios.

3.6.1 DCB test - mode I fracture toughness of CFRP

Specimen preparation

The DCB specimen is prepared considering 8 plies of unidirectional $0°$ layups of carbon fibre(200GSM), epoxy CY 230-1 and hardener HY-951 according to the ASTM D5528 standard. The aluminium foil is inserted along the mid-plane of the laminate to create a delamination length of 50 mm. The foil is coated with wax on both the sides so that it does not stick with the laminae. The dimensions of the DCB specimen are given in the Table 3.2. The rest of method used for specimen preparation is same as described in the section 3.2.1. The schematic of the DCB specimen is shown in the Fig3.16.
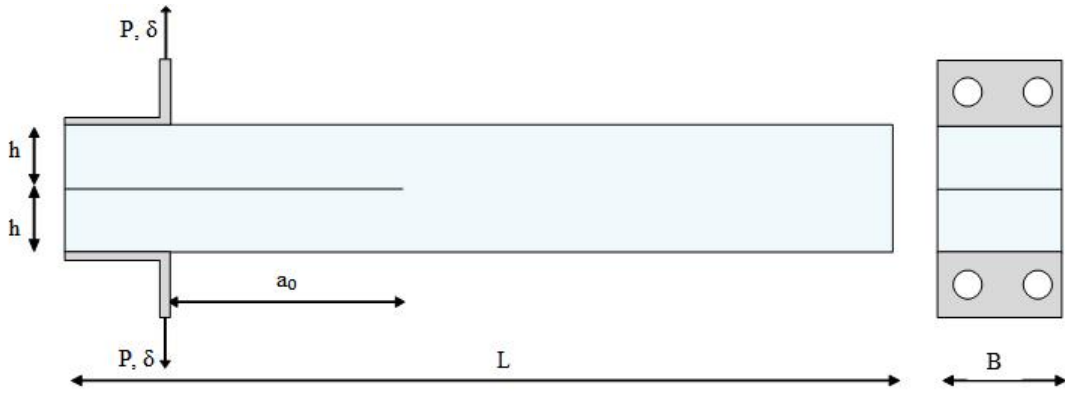
Figure 3.16: Schematic representation of DCB specimen

Mode I fracture toughness calculation

The experimental method followed is same as the method used for DCB test in the previous section. From experimental load versus displacement curve it can be observed that, after reaching maximum load value delamination starts and therefore load curve starts dropping. The DCB specimen with the given dimensions is modelled in the ANSYS15. The number of simulations are performed to get the match between experimental and numerical load-displacement curve. SIF at the crack tip is matched with the SIF obtained from experimental data. Also, the simulations are performed at initial delamination length of 30 mm and 40 mm. The curves obtained from these simulations are used for fracture toughness calculations.
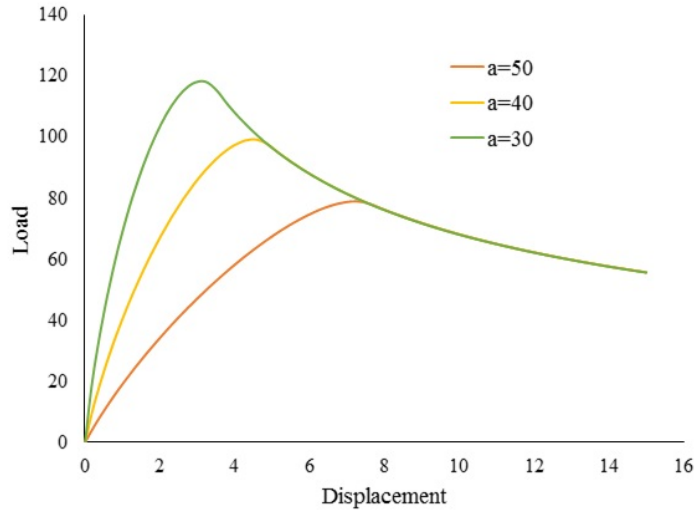
Figure 3.17: Load vs displacement curve for 3 delamination lengths: 30, 40 and 50

In this study, compliance beam theory with equivalent crack length is used. The strain energy release rate is calculated as follows:

$$G_I = \frac{6P^2}{B^2 h} \left(\frac{2a_e^2}{E_f h^2} + \frac{1}{5G_{13}} \right) \tag{3.16}$$

35
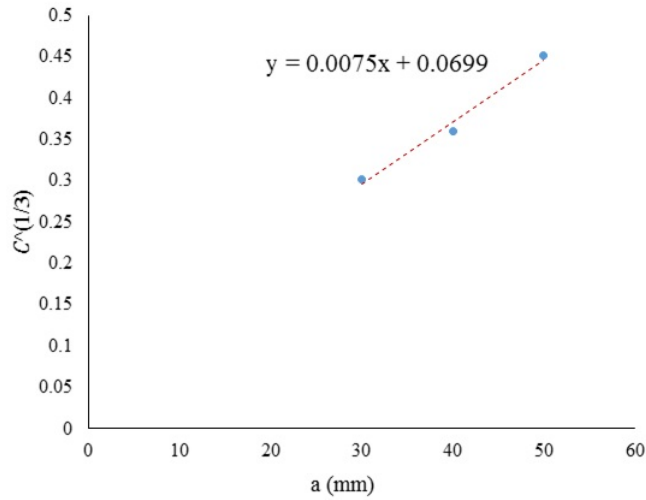
Figure 3.18: Compliance beam theory for fracture toughness of CFRP

The above expression overestimates the fracture toughness value. To account for that consider crack length correction. Δ can be determined by generating least squares plot of the cube root of compliance, $C^{1/3}$, as a function of delamination length. Compliance is the ratio of displacement to the applied load. Crack length correction corresponds to the intercept of the line fitted to the 3 data points as shown in the Fig 3.18. The equation is:

$$y = 0.0075x + 0.0699$$

Δ is found out as 9.32 mm. The equivalent crack method is used to obtain R-curves.
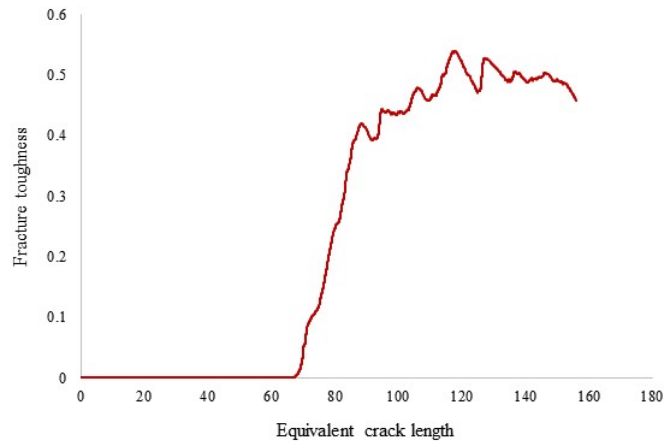
Figure 3.19: R curve for DCB specimen

The equivalent crack method is used to get the R-curve for a specimen as shown in the Fig3.19. In the images obtained from DIC, the location of initial crack tip was identified. The pair of points to calculate CTOD was selected on left and right side of the crack tip location. To extract the cohesive law from the experiments, plot the curve fracture toughness vs crack tip opening displacement.
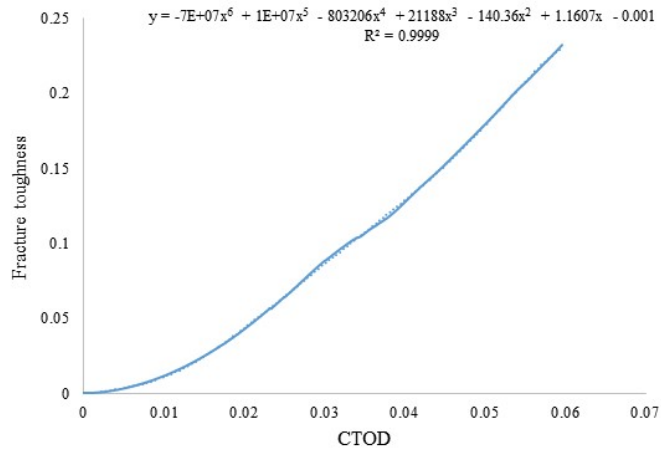
Figure 3.20: G-CTOD relation for DCB specimen

After that, fit the six degree polynomial to the curve as shown in the Fig 3.8. The equation is:

$$y = -970.01x^6 + 1501x^5 - 768.72x^4 + 138.1x^3 - 1.399x^2 + 0.3381x - 0.0004$$

Differentiate the with respect to CTOD to get the relation between traction and crack tip opening displacement. Plot the traction equation against CTOD. That will give the traction-separation law for the given case as shown in the Fig 3.21.
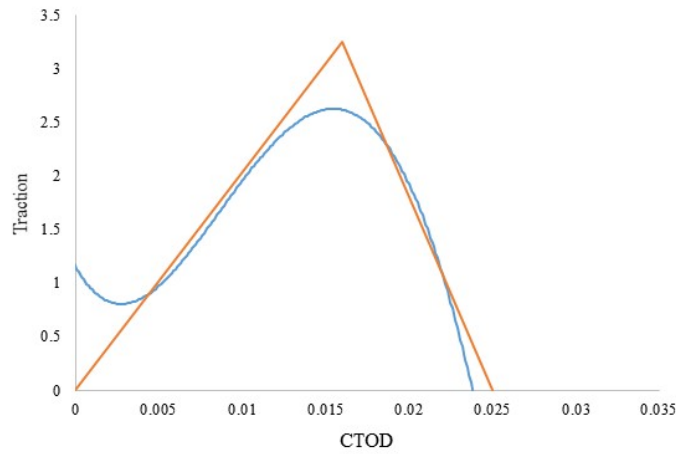
Figure 3.21: Mode I cohesive law for CFRP

The mode I fracture parameters for the adhesive are given in the Table 3.10 as obtained through the experiment.

Table 3.10: Cohesive law parameters obtained from experiment: Mode I

Parameter	Value
Mode I fracture toughness	0.041 N/mm
Maximum normal traction	3.25 N
Normal separation	0.025 mm

3.6.2 ENF test - mode II fracture toughness of CFRP

Specimen preparation
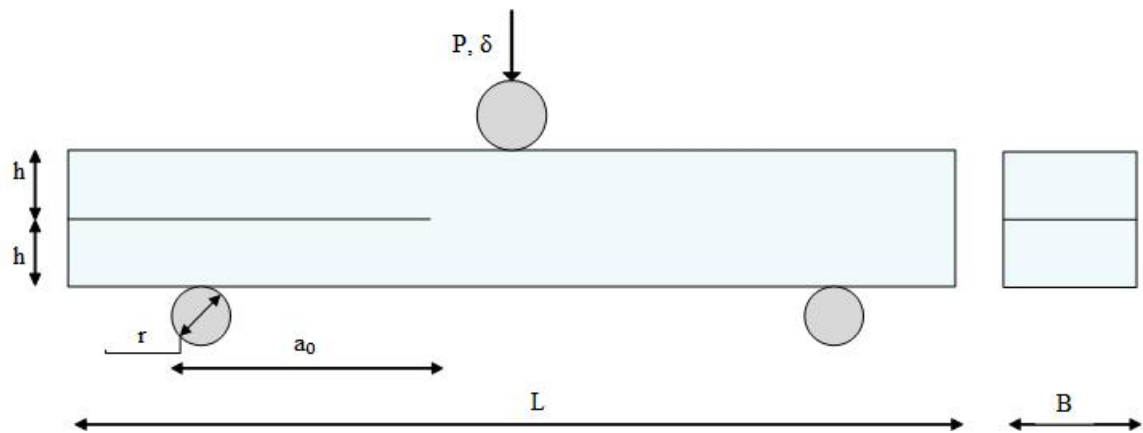
Figure 3.22: Schematic representation of ENF specimen

The method used in ENF specimen preparation is same as the method used for DCB specimen preparation as described in previous section. The schematic of ENF specimen is as shown in the Fig3.22 and dimensions are mentioned in Table3.7.

Mode II fracture toughness calculation

The experimental load vs displacement curve for the three tested specimens is shown in the Fig 3.23. From the curve it can be observed that, after reaching maximum load value delamination starts and load starts dropping. The interlaminar mode II fracture toughness can be calculated by using compliance calibration (CC) method as mentioned in ASTM D7905[28].
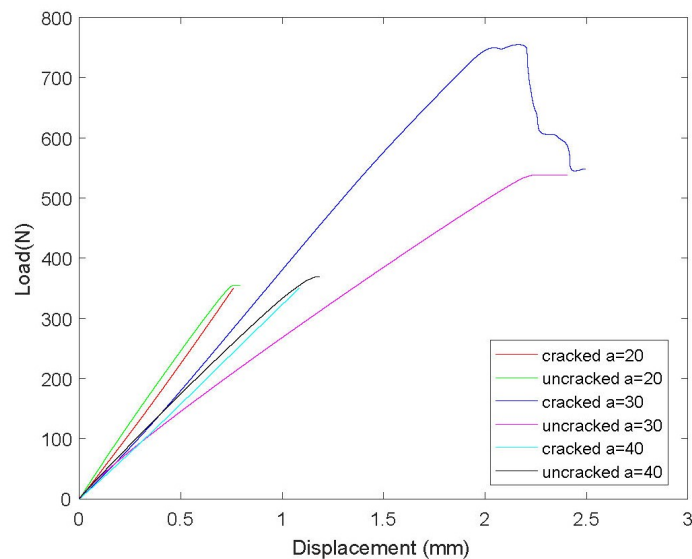
Figure 3.23: Load-displacement curves for ENF specimen

G_{IIc} will be the minimum of the values calculated from PC and NPC tests. From load-displacement curve, stiffness of the specimen can be found out. Compliance is a reciprocal of stiffness. Plot the graph of compliance vs cube of delamination length. Compliance in ENF is directly proportional to the cube of delamination length as shown in Fig 3.24. Fit the curve for the equation below:

$$C = A + ma^3$$

A and m are compliance calibration coefficients. The value of compliance calibration coefficient are obtained as A = 0.0021 and m = 2×10^{-8}.
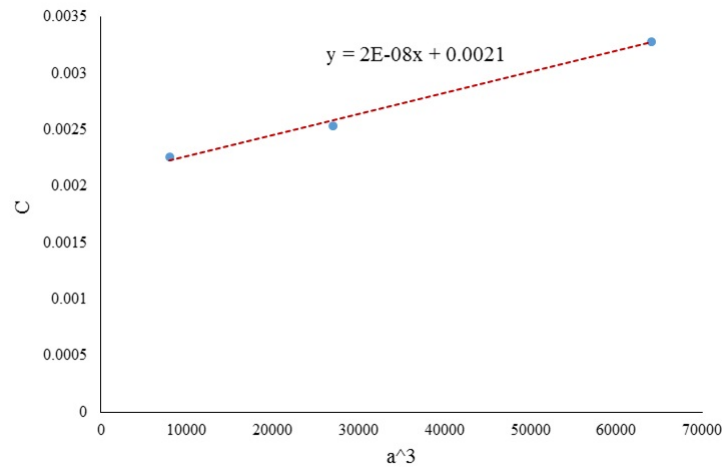
Figure 3.24: Compliance vs a^3 curve for ENF specimen

The fracture toughness can be calculated as

$$G_{IIc} = \frac{3mP_{max}^2 a^2}{2B} \tag{3.17}$$

Mode II fracture toughness for all specimen is calculated using the above equation. The result is given in the Table 3.11.

Table 3.11: Mode II fracture toughness

Specimen	1	2	3	4	Average
G_{II}	0.844	0.615	0.673	0.715	0.711

3.7   Conclusion

In this chapter, cohesive zone model for adhesive and CFRP is presented. This model is derived for mixed-mode delamination in case of static loading condition. Experimental characterisation is done for interlaminar fracture toughness of araldite 2015 for CFRP specimen under mode I and mode II loading. Mode I fracture toughness is obtained as 0.44 N/mm. It is calculated using compliance beam theory with equivalent crack method. The mode II fracture toughness is obtained as 2.76 N/mm. It is calculated using compliance calibration method. The formulation is implemented in FEA to get the characteristic parameter of material for mixed-mode delamination. For the given case it is found out to be 3.

Similar experiments are performed to get the interlaminar fracture toughness of CFRP panel. Mode I fracture toughness is obtained as 0.921 N/mm. It is calculated using compliance beam theory with equivalent crack method. The mode II fracture toughness is obtained as 0.711 N/mm. It is calculated using compliance calibration method. MMB test is performed to characterise mixed-mode delamination.

Chapter 4

Delamination modelling in unidirectional CFRP Laminate under static loading using FEA

4.1   Introduction

Adhesives are commonly used to bond structural component into assemblies or to bond layers of materials into composite laminates. Simulations are performed to model the progressive separation of the adhesive as it reaches critical stress limit. Mechanical APDL supports two methods i.e. cohesive zone model and virtual crack closure technique to define the failure criteria. In these methods, separation occurs along predefined interface. In this thesis, cohesive zone model has been used to simulate the separation mechanism of two surfaces. There are two methods to represent interface surfaces of the material: i) Interface elements and ii) Contact elements.

Interface elements
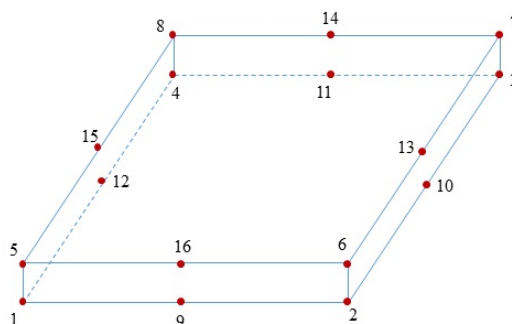
Figure 4.1: 3D 16-node interface element

   The interface elements represent the cohesive zone between the components and they account for the separation across the interface. It is a zero thickness element. Interface failure is detected

by elemental traction and separation. An interface element is composed of bottom and top surfaces. Fig4.1 shows a 3-D 16-node quadratic interface element.

Contact elements

The cohesive zone between components can be modelled with bonded contact. One surface is treated as contact surface and other is treated as target surface. Interface separation is detected by separation of contact and target surfaces and it is defined in terms of contact gap and tangential slip distance.

4.2   FEM modelling of DCB test

3D Finite element model is developed using finite element package, ANSYS 15. To model a DCB specimen with length 130 mm and width 25 mm, solid186 element is used. It is a 20-noded brick element. This specimen has 8 layers giving total thickness of 4 mm. In x-y-z coordinate system, length, width and the thickness of the specimen are oriented in x, z, and y-direction respectively. The mesh pattern in the ligament portion is kept finer as compared to the cracked portion to capture the accurate delamination process. The mesh parameters for the model are given in the Table 4.1. As discussed in section 3.3.3 the length of cohesive zone element is 0.637 mm. Here, we have taken length as 0.5 mm to be on safer side. Material properties mentioned in the Table 3.1 are applied to the specimen. To simulate the DCB test condition, one end of the specimen is fixed and at the other end displacement is applied.

Figure 4.2: Finite element model for DCB test

Table 4.1: Mesh parameters for DCB specimen

Dimension	Number of elements
Ligament length	144
Cracked length	29
Width	25
Half-thickness	4

4.2.1 Interface elements modelling

In-built CZM model with actual crack length

The ligament length in the model represents the bonded part of the DCB specimen. To simulate delamination, interface elements INTER204 are i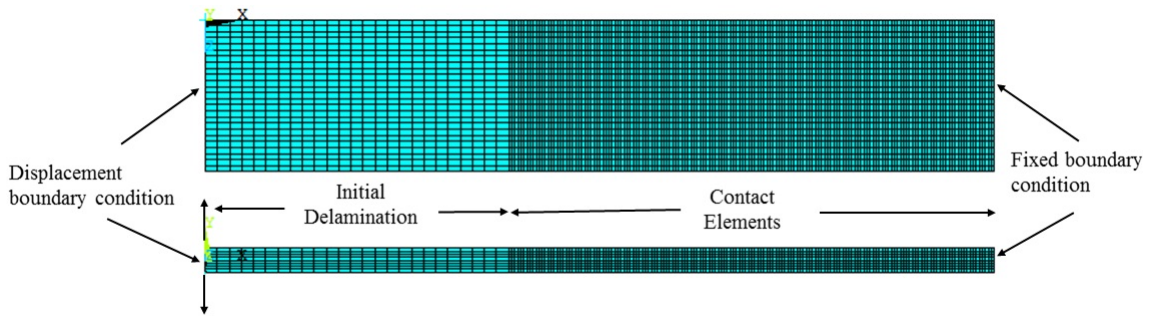ntroduced along the ligament length. The geometry of the standard interface element with 16 nodes is shown in the Fig 4.1. The initial delamination length is taken as 50 mm. The cohesive zone model is implemented through in-built bilinear cohesive zone model. The properties of the cohesive zone are defined in the Table 4.2. The load-displacement curve for the finite element model with actual crack length is shown in the Fig. **??**.

Table 4.2: Cohesive zone properties for in-built bilinear model

Material property	Value
Mode I fracture toughness,G_{Ic}	0.45 N/mm
Mode II fracture toughness,G_{IIc}	2.75 N/mm
Mode I interfacial strength, T_n	2.76 MPa
Mode II interfacial strength, T_t	25 MPa
Ratio of onset separation to normal separation, α	0.00174

4.2.2 Contact pair modelling

To model the cohesive zone along the ligament length contact pair is used. For simulation, surface to surface CONTA174 elements are used along with TARGE170 elements. Contact pair consists of one contact surface and one target surface. Four different contact algorithms are available in APDL which are pure penalty method, augmented lagrangian method, pure lagrange multiplier method and lagrange multiplier on contact normal and penalty on frictional direction. Here augmented lagrangian method is used. It is an iterative series of penalty updates and is less sensitive to the magnitude of the contact stiffness coefficient. The contact tractions are augmented during iterations. The equilibrium iterations are continued till final penetration is less than allowable tolerance. Contact parameters required to define the contact pair are defined in Table4.3. Numerical simulations are performed using inbuilt and user defined model. The inbuilt cohesive zone law uses CBDE. It describes the bilinear material behaviour with tractions and separation.

Table 4.3: Contact pair parameters for DCB test model

Parameter	Value
Contact algorithm	Augmented lagrange method
Contact detection	At nodal point
Contact stiffness factor	1.0
Penetration tolerance factor	0.1
Pinball region factor	0.5
Contact stiffness update	At each iteration
Initial gap	Included
Contact adjustment	Initially closed

4.2.3 Result and discussion

The load-displacement curve obtained by interface elements shows a match with the curve obatined by contact elements. The disparity between the numerical and experimental curves is either due to inaccurate measurement of the physical crack or due to modelling mixed mode delamination as pure mode I delamination. For modelling DCB specimen two methods are used: (a) Modified cohesive mode I crack method and (b) Benzeggagh-Kenane model. These two methods are subsequently discussed at length in this chapter.
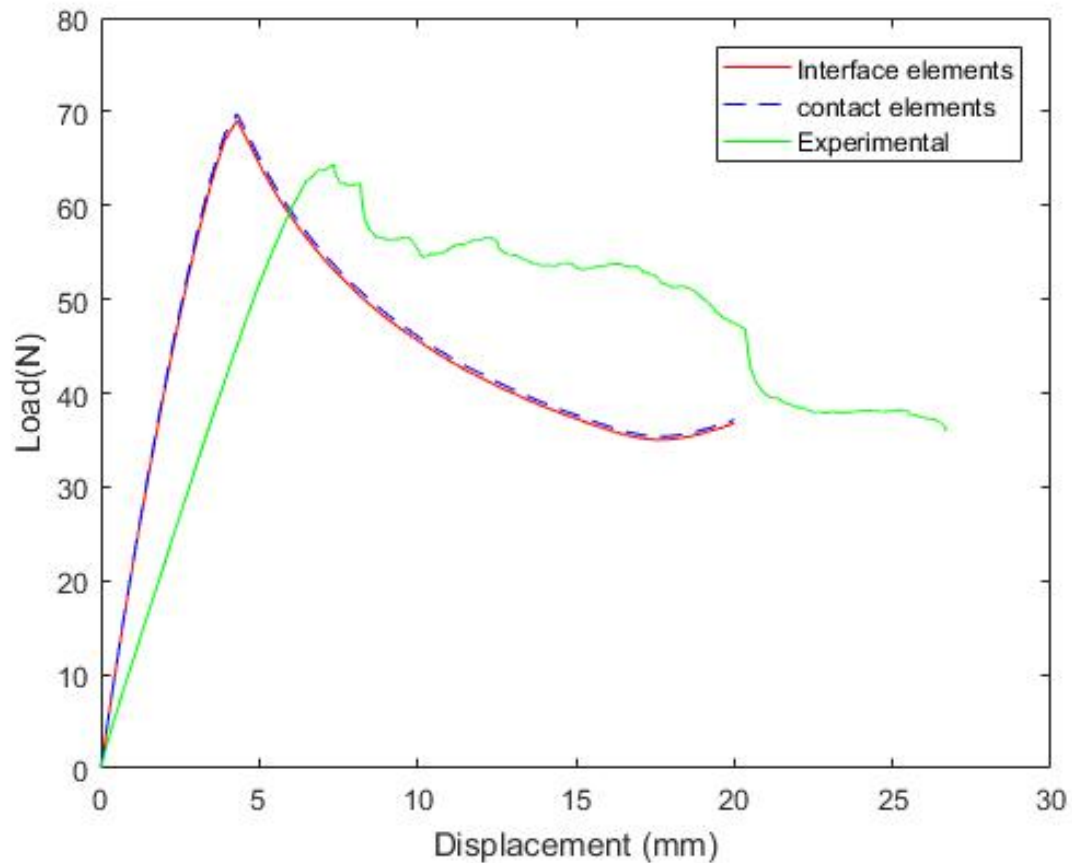
Figure 4.3: Load-displacement curve for DCB specimen using interface modelling and contact pair modelling

Interface elements vs. Contact elements

Previously we have discussed the two methods which are used to represent interface surface of the material. The results obtained by interface elements shows match the result obtained by contact elements. Interface elements are not able to show actual material separation. In contact elements, actual material separation is observed by debonding the interface surfaces. The main problem with contact elements is that the contact algorithms in FEA are complicated and thus it takes much longer time to get the converged solution. Interface elements are easy to implement and it takes

less time to get converged solution. To visualise and model the actual material separation, contact elements are used in this thesis for further study.

4.2.4 Method 1 - Modified cohesive mode I crack

The modelling details of DCB specimen are same as in the previous case and cohesive zone properties are given in the table 4.2. In the section 3, effective crack length evaluation from SIF estimator has been discussed. The effective crack length obtained is 58 mm. Simulations are performed considering the effective crack length of the specimen. The load-displacement curve obtained is shown in the Fig 4.6.

4.2.5 Method 2 - Benzeggagh and Kenane model

To consider for mode-mixity, mixed mode cohesive zone model is implemented through user programmable subroutine function. The formulation is based on the method developed by Benzeggagh and Kenane[24]. The properties of the user defined cohesive zone are given in the table 4.4.

Table 4.4: Cohesive zone properties for UserCZM model

Material property	Value
Mode I fracture toughness,G_{Ic}	0.45 N/mm
Mode II fracture toughness,G_{IIc}	2.75 N/mm
Mode I interfacial strength, T_n	2.76 MPa
Mode II interfacial strength, T_t	25 MPa
Penalty stiffness, K	1000 N/mm
Mode interaction parameter, η	3

4.2.6 Result and discussion

Fig. 4.4 shows the contact gap distance for DCB specimen of CFRP panel. In the figure, blue rgion represents the complete material separation and red region indicates bonded contact. Fig. 4.5 shows contact stress distribution for the boundary value problem shown in the Fig. 4.2. In the figure, nagative contact stress indiacates completely separate region and positive contact stress represnets bonded contact. The maximum contact stress is observed at fixed end of the specimen and its value is 2.717 N/mm^2. The load-displacement curve is obtained as shown in the Fig. 4.6.

Figure 4.4: Contact gap for DCB specimen

Figure 4.5: Contact stress for DCB specimen
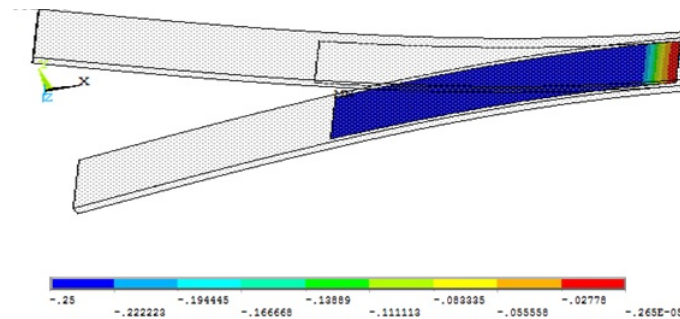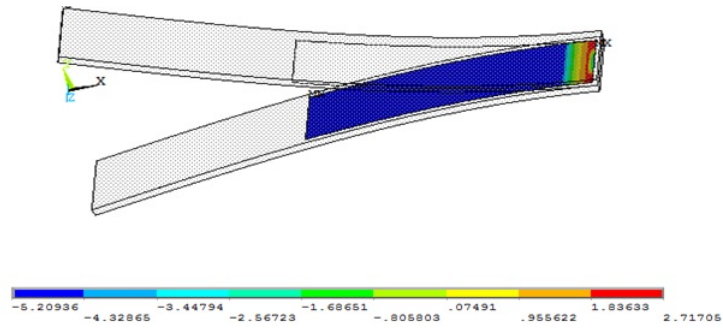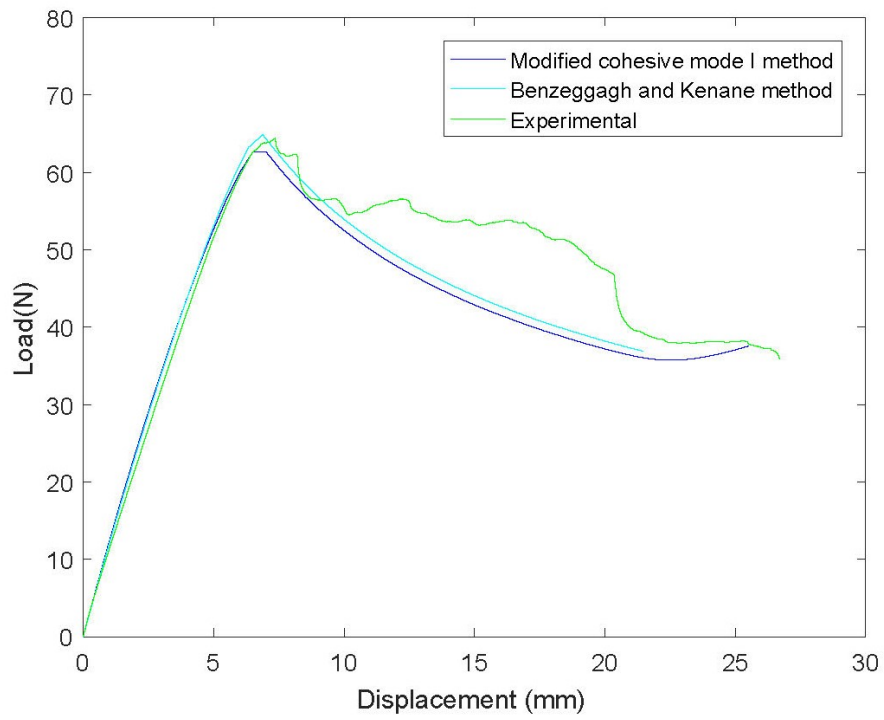

Figure 4.6: Load-displacement curve for DCB specimen using contact modelling

4.3   FEM modelling of ENF test

3D Finite element model is developed using finite element package, ANSYS15. ENF specimen with length 165 mm and width 25 mm is modelled using the same method as used for DCB specimen. This specimen has 8 layers giving total thickness of 4 mm. The mesh parameters used are given in Table 4.5.
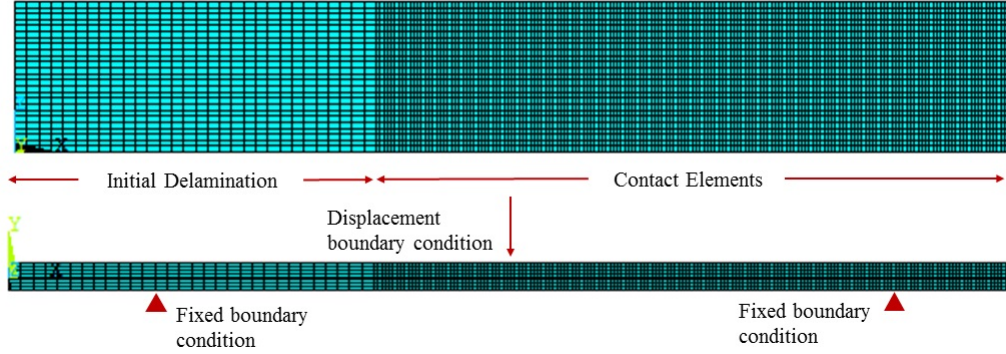
Figure 4.7: Finite element model for ENF test

Table 4.5: Mesh parameters for ENF specimen

Dimension	Number of elements
Ligament length	168
Cracked length	30
Width	25
Half-thickness	4

4.3.1   Contact pair modelling

To model the cohesive zone along the ligament length contact pair is used. For simulation, surface to surface CONTA174 elements are used along with TARGE170 elements. There are two contact pairs created. One contact pair for cracked region and one for ligament region. Each contact pair consists of contact surface and target surface. Out of the four available contact algorithms, augmented lagrangian is used here. The contact parameters for the two pairs are given in the table 4.6.

Table 4.6: Contact pair parameters for ENF test model

Parameter	Contact pair 1	Contact pair 2
Contact algorithm	Augmented lagrangian	Augmented lagrangian
Contact detection	At gauss point	At nodal point
Contact stiffness factor	0.1	0.000683
Penetration tolerance factor	0.05	0.05
Pinball region factor	2	0.25
Contact stiffness update	At each iteration	At each iteration
Initial gap	Included	Included
Contact adjustment	Initially closed	Initially closed

4.3.2 Results and discussion
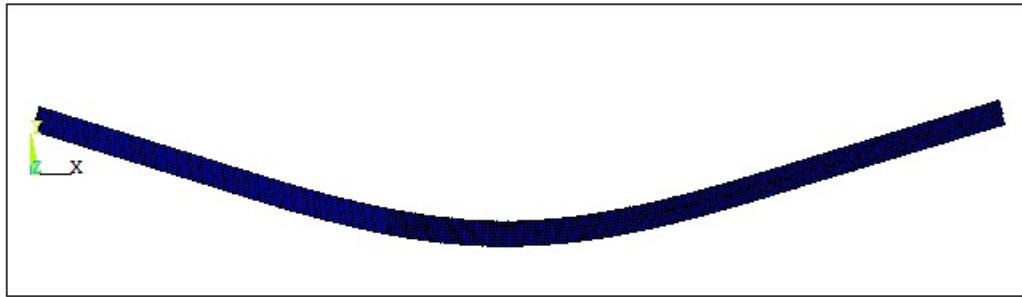
Figure 4.8: Deformed shape of ENF specimen using contact modelling

The deformed ENF specimen using contact pair modelling is shown in the Fig 4.8. Fig 4.9 shows the contact gap distance and Fig 4.10 contact stress distribution for the boundary value problem shown in the Fig 4.7. The load-displacement curve is obtained as shown in the Fig 4.11.
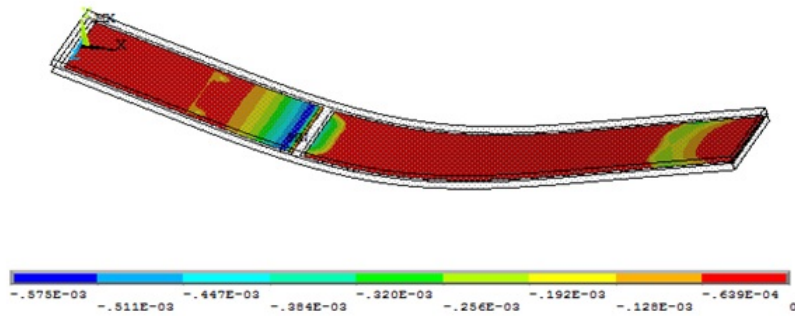
Figure 4.9: Contact gap for ENF specimen
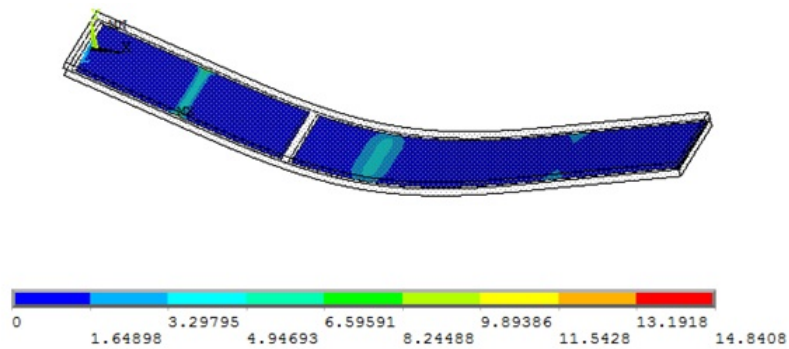
Figure 4.10: Contact stress for ENF specimen
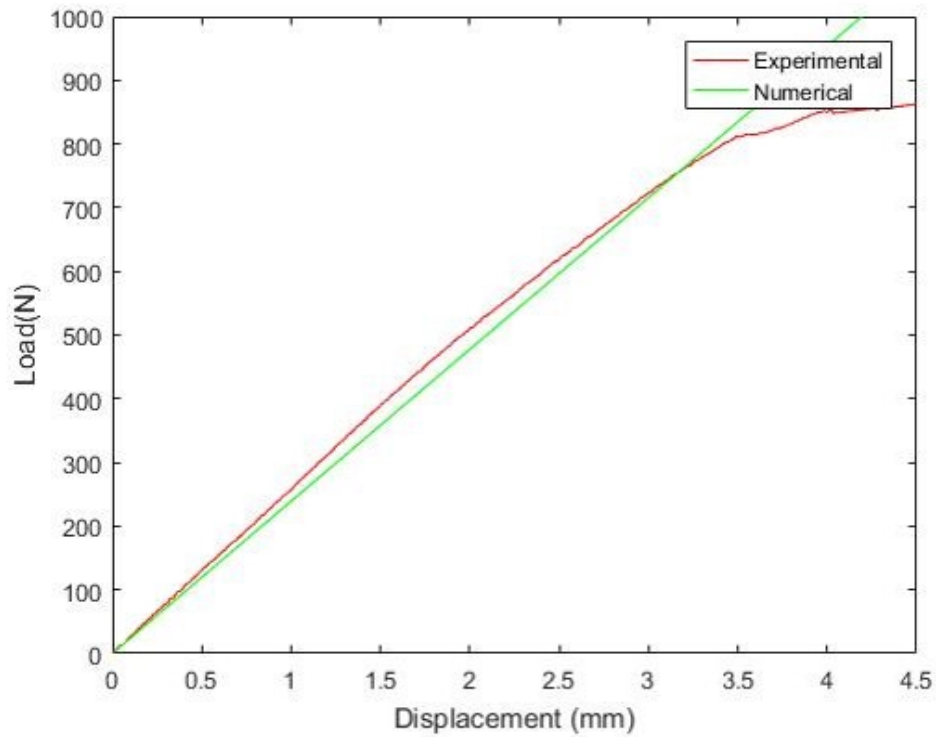
Figure 4.11: Load-displacement curve for DCB specimen using contact modelling

4.4 Conclusion

In this chapter, numerical study is carried out to and the results obtained are validated with the experiments performed. Here, both DCB and ENF specimen are studied. Two methods namely, interface modelling and contact pair are compared and contact pair method is selected for its advantages. The load-displacement curves obtained with user developed cohesive zone model for both the specimen are found to be in close match with experimental results.

Chapter 5

Analysis of single and double stepped lap joint of CFRP laminate under tensile loading

5.1   Damage repair in composites

The damage in the composite reduces the strength of the structures which is associated to the recycling difficulties and replacement costs[1]. It is more ecologically efficient to repair the structures than replacing them[23]. The repair of structure with composite patch can be carried out in two ways: i) Mechanical fastening or ii) adhesive bonding. Mechanical fastening method includes the use of connectors such as rivets, bolts and nuts. The main disadvantage with their use is that they result in high stress concentration and galvanic corrosion. This can be avoided by using adhesively bonded repairs and the benefits associated with it are improved appearance, good sealing properties, high strength to weight ratio and reduced stress concentration[1, 22]. There are different types of boded joints such as: single lap joints, scarf joints, tapered joint and stepped-lap joints.

The schematic for different types of repair is shown in the Fig 5.1. Scarf joint repair involves the removal of damaged area by drilling a hole and then adhesively bonding the patch layers to fill the damaged portion. A step lap joint is similar to the scarf joint. The only difference is that it has a series of uniform steps that form taper. A stepped-lap bonded joint is generally used in composite structure with thickness more than 4mm, as the load transfer through step-lap joint is more uniform through shear loading. Scarf joint panel behaviour is complex as compared to stepped lap joint.

In this work, analysis of single and double sided stepped lap joint of CFRP laminate under tensile load is studied. Experimental results for the same are compared with a numerical estimates. The cohesive law for the adhesive interface with CFRP is determined for mode I and mode II loading conditions experimentally. This cohesive law is given as input to the FEA fot estimating the mechanical behaviour of bonded stepped lap CFRP laminate under tensile loading condition.
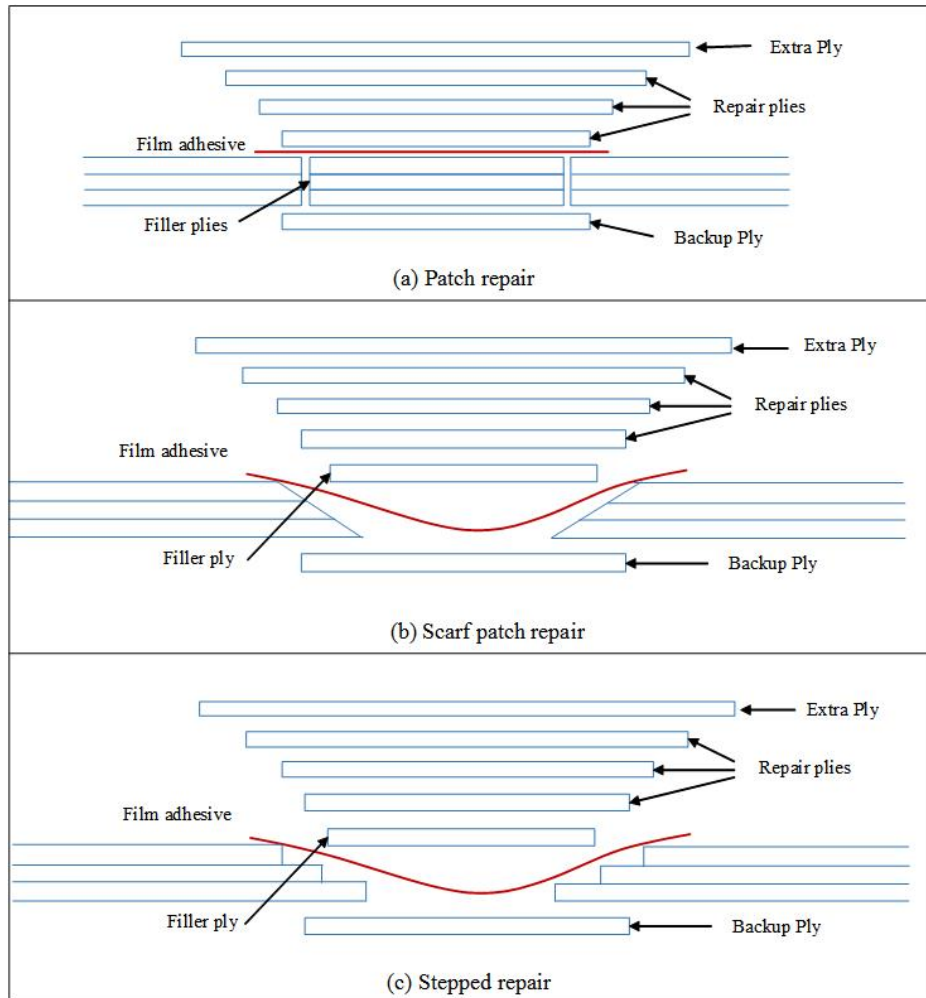
Figure 5.1: Different forms of Composite damage repairs

5.2 Analysis of single stepped lap joint

5.2.1 Specimen preparation

The CFRP laminates for single sided stepped lap joint specimen are prepared from unidirectional carbon fibre mat of 200 gsm weight through vacuum bagging procedure. The matrix is composed of epoxy resin CY 230 and hardener HY 951 in proportion of 10:1 by weight ratio. The plates were cured at room temperature with a curing time of 24 hours. The panel is made of 8 unidirectional layers. The carbon fibre fabric layers were stacked in the 0° direction. The bonding surfaces of the specimen are roughened using emery paper and then cleaned with acetone. A ductile epoxy adhesive is used to bond the two parts at room temperature. A constant thickness of 0.2 mm was ensured for the adhesive layer. The schematic of the specimen is shown in the Fig 5.2 and the dimensions of the specimen are given in the table 5.1. Random speckle pattern is created on thickness side of the specimen to measure displacements through DIC.

Table 5.1: Dimensions of single stepped lap joint of CFRP panel

Dimension	Value
Overall length (L)	140 mm
Free length (l_f)	45 mm
Width (B)	45 mm
Thickness (h)	2.6 mm
Step height (h_s)	0.52 mm
Step length (l_s)	12.5 mm
Taper angle (α)	1°
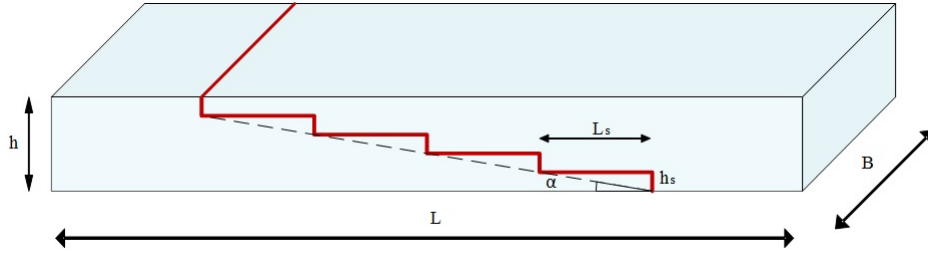
Figure 5.2: Schematic representation of single stepped lap joint of CFRP panel

5.2.2 Experimental setup
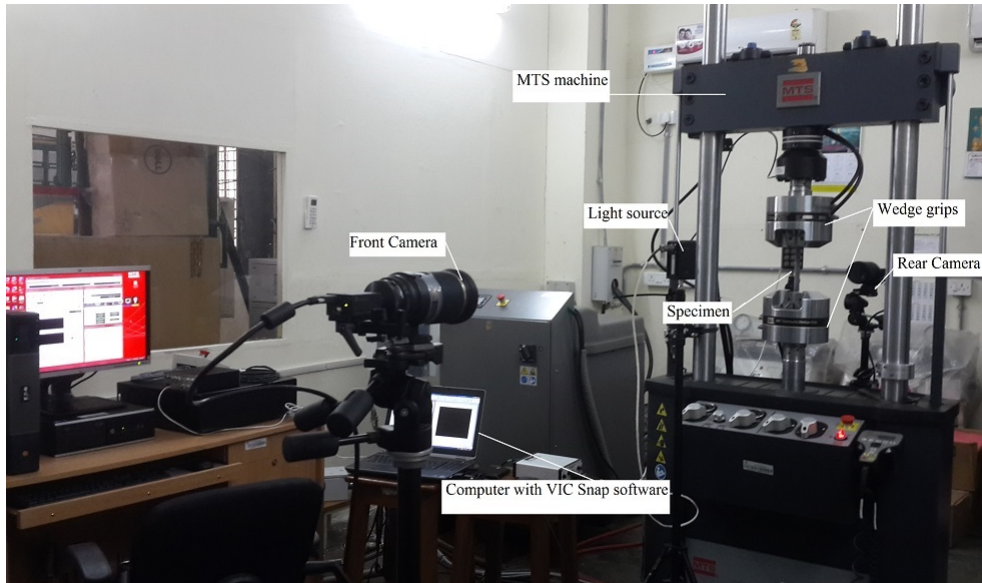
Figure 5.3: Experimental setup for testing single stepped lap joint in a CFRP laminate

Experimental setup for the single stepped lap joint test is shown in the Fig. 5.3. The experiment is performed on 100kN MTS universal testing machine. 2D-DIC system is used to track the through the thickness full displacement and strain field. It has single Grasshopper CCD camera with a spacial resolution of 2448 x 2048 pixels. Tamron lens is used to capture the entire length of the specimen. Camera is mounted on tripod and aligned with the specimen so that it can capture the images accurately. Two white light LED sources are used on both the sides of camera to ensure

the proper illumination of the specimen. The tensile load is applied at a loading rate of 1mm/min and the load displacement data is obtained. Five images are captured per second and stored in a computer using Vic 2D software.

5.2.3 Finite element analysis

Finite element analysis of single stepped lap joint in CFRP panel under tensile loading condition is carried out in FEA software ANSYS 15. To model a single stepped lap CFRP panel with length 140 mm and width 45 mm, solid 186 element is used. This specimen is modelled with 8 unidirectional layers and total thickness of 2.6 mm. Adhesive layer is modelled using contact elements. TARGE170 and CONTA174 elements are used to represent contact pair and the contact algorithm used is augmented lagrangian. In XYZ coordinate system, length, width and the thickness of the specimen are oriented in x, z, and y direction respectively. The CFRP panel is fixed at bottom edge and centre node is fixed to avoid the motion in the normal direction. Along the x-direction at the top edge tensile load is applied. Finite element model for a single stepped lap CFRP panel is shown in the Fig 5.4. The mesh parameters for the model are given in the table 5.2. Material properties mentioned in the table 3.1 are applied to the specimen.
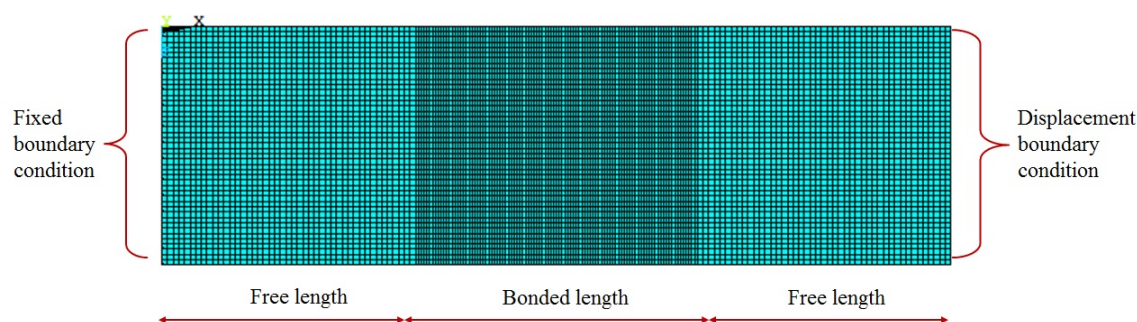
Figure 5.4: Finite element model of single stepped lap joint of CFRP panel

Table 5.2: Mesh parameters for single stepped lap joint of CFRP panel

Dimension	Number of elements
Free length	30
Step length	60
Width	15
Step height	2

To model the cohesive zone along the bonded length contact pair is used. For simulation surface to surface CONTA174 elements are used along with TARGE170 elements. Contact pair consists of one contact surface and one target surface. Out of the four available contact algorithms, augmented lagrangian is used. Contact parameters required to define the contact pair are defined in Table 5.3. Numerical simulations are performed using user defined cohesive zone model. It describes the bilinear material behaviour. The cohesive zone properties for UserCZM model are given in Table 4.4.

Table 5.3: Contact pair parameters for a single stepped lap joint of CFRP panel test model

Parameter	Value
Contact algorithm	Augmented lagrange method
Contact detection	At nodal point
Contact stiffness factor	1.0
Penetration tolerance factor	0.1
Pinball region factor	0.5
Contact stiffness update	At each iteration
Initial gap	Included
Contact adjustment	Initially closed

5.2.4   Results and discussion

Local behaviour:

The Fig. 5.5 shows the contact gap distance for single stepped lap joint of CFRP panel. In the figure, red region represents the contact distance of 0. The contact and target surfaces are still in contact with each other. The delamination process starts at the step height. After completion of delamination at step height, delamination starts along the length. In the length direction, delamination starts in the first and last step. The onset point is 0.0027 mm and the region indicating green-blue area is already separated. Delamination front is travelling towards the centre.
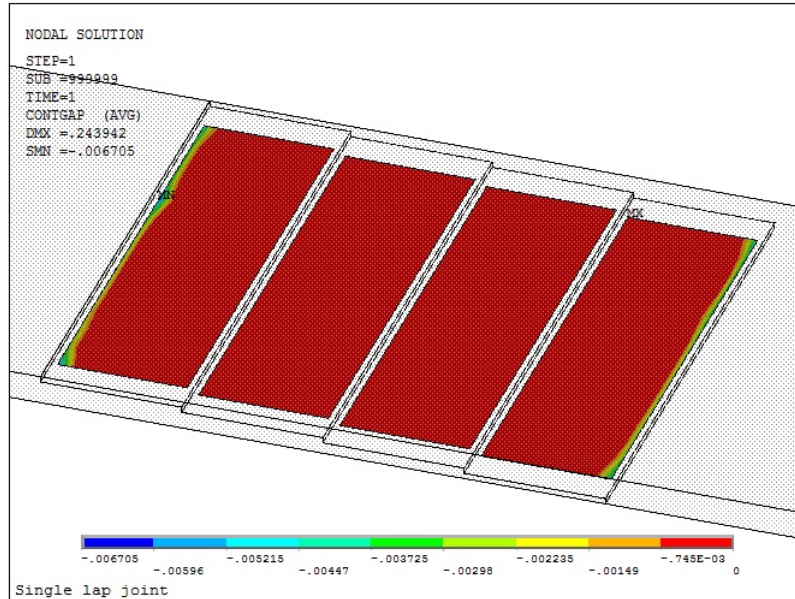
Figure 5.5: Contact gap distance for single stepped lap joint of CFRP panel

The Fig. 5.6 shows the contact stress for single stepped lap joint of CFRP panel. In the figure, contact stress 0 indicates bonded region. At both the ends of step length, light blue region is observed indicating the start of the delamination process. The maximum stress is observed at the first step and the value is 288.29 N/mm^2.
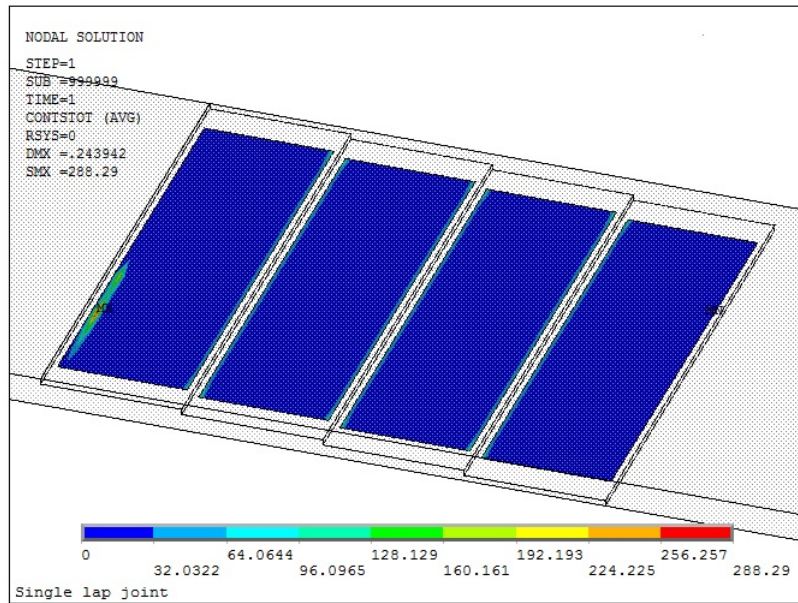
Figure 5.6: Contact stress for single stepped lap joint of CFRP panel

Global behaviour:

The load-displacement curve is obtained as shown in the Fig 5.7. The load transfer between the adherends is by shear deformation mechanism. The failure starts near the step corners and then propagates towards the centre of the step. Ultimate failure of the CFRP panel occurs along the adhesive layer and panel splits into two. Load-displacement data obtained by experiment and numerical method shows good match.
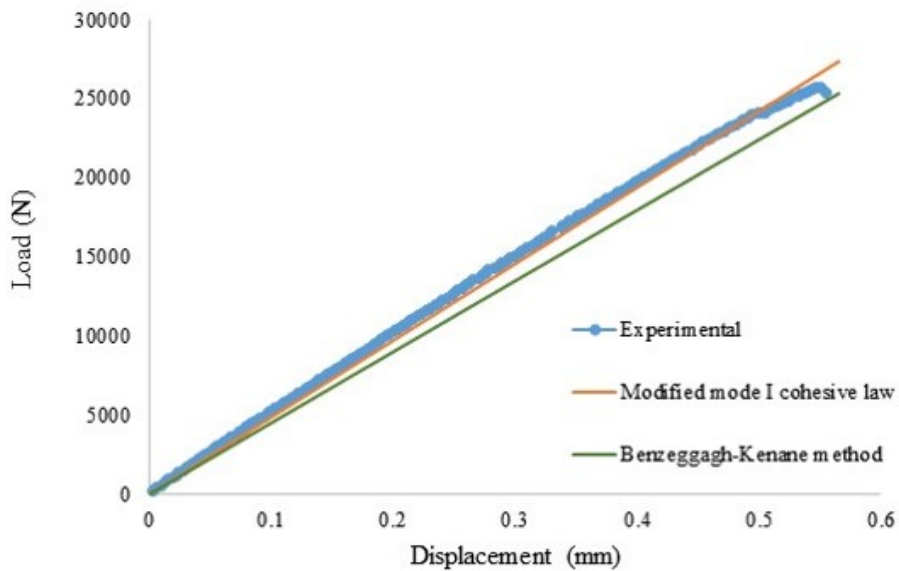
Figure 5.7: Load-displacement curve for single stepped lap joint of CFRP panel using contact modelling

5.3 Analysis of double stepped lap repair

5.3.1 Specimen preparation

The rectangular laminate plate with three layers is made of CFRP composite with the fibre orientation of 0° along x-axis. CFRP laminates are prepared from unidirectional carbon fibre mat of 200 gsm weight through vacuum bagging procedure. The matrix is composed of epoxy resin CY 230 and hardener HY 951 in proportion of 10:1 by weight ratio. The plates were cured at room temperature with a curing time of 24 hours. The laminate is made up of 12 unidirectional layers. The mechanical properties of CFRP are given in the table 3.1. The bonding surfaces of the specimen are roughened using emery paper and then cleaned with acetone. A ductile epoxy adhesive is used to bond the two parts together. A constant thickness of 0.2 mm was ensured for adhesive layer. The schematic of the specimen is shown in the Fig 5.8 and the dimensions are given in the table 5.4. Random speckle pattern is created on thickness side of the specimen to measure displacements through DIC.

Table 5.4: Dimensions of double stepped lap joint of CFRP panel

Dimension	Value
Overall length (L)	220 mm
Width (B)	45 mm
Thickness (h)	2.4 mm
Step height (h_s)	0.8 mm
Step length (l_s)	13 mm
Adhesive thickness (t)	0.2 mm
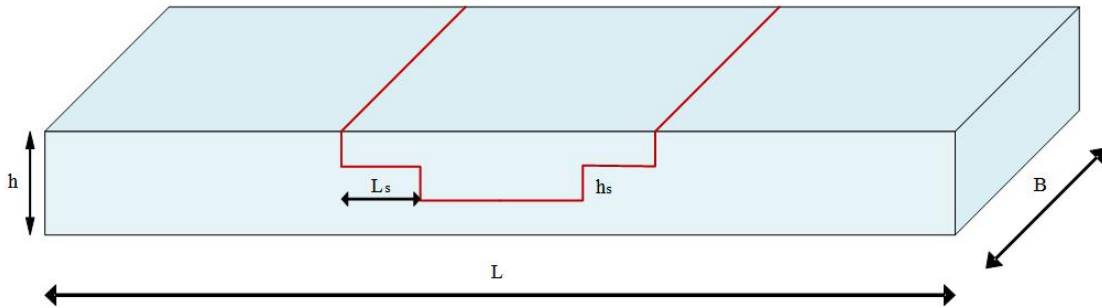
Figure 5.8: Schematic representation of double stepped lap joint of CFRP panel

5.3.2 Experimental setup

The experimental setup is same as used for the single stepped lap joint test.The experimental setup consists of 100 kN MTS universal testing machine. Experimental setup for the tensile testing of double stepped lap joint is shown in the fig 5.3. 2D-DIC system is used to track the through the thickness full displacement and strain field. The system consists of single CCD camera having spatial resolution of 2448 x 2048 pixels coupled with tamron lens. Camera is mounted on the tripod and aligned with the specimen so that it can capture the images accurately. Magnified optics involving InfiniProbe TS-160 lens is used to capture the local strain over the adhesive layer closer to step

corners. It gives magnification range of 0-16X. Two white light LED sources are used on both the sides of camera to ensure the proper illumination of the specimen. The tensile load is applied at a loading rate of 1mm/min and the load displacement data is obtained. Five images are captured per second and stored in a computer using Vic 2D software.

5.3.3 Numerical analysis

Finite element analysis of double stepped lap joint in CFRP panel under tesnile loading condition is carried out in FEA software ANSYS 15. The cohesive law defined in the previous sections is used for the analysis. The cohesive zone parameters used for simulations are given in the table 4.4. The CFRP laminate is modelled with a 12 unidirectional layers. Total thickness of the specimen is 2.4 mm and step height is 0.8 mm. The specimen is modelled such that each step consists of 4 UD layers. The mechanical properties for the CFRP are given in the table 3.1. The specimen of the model are same as the experimental specimen. 20 noded brick element, SOLID186 is used to model the laminates and adhesive layer is modelled using contact elements. TARGE170 and CONTA174 elements are used to represent contact pair and contact pair consists of one contact surface and one target surface. Out of the four available contact algorithms, augmented lagrangian is used. Contact parameters required to define the contact pair are defined in Table 5.3. The length of the cohesive zone is determined to be 3.185 mm based on the formulation defined by Turon. To obtain accurate FEM results using CZM, it is recommended to use five elements in the cohesive zone. Considering this, the mesh size in the adhesive layer is taken as 0.5 mm. In XYZ coordinate system, length, width and the thickness of the specimen are oriented in x, z and y direction. The CFRP panel is fixed at bottom edge and centre node is fixed to avoid the motion in the normal direction. Along the x-direction at the top edge tensile load is applied. Finite element model for a double stepped lap CFRP panel is shown in the Fig 5.9. The mesh parameters for the model are given in the table 5.5.
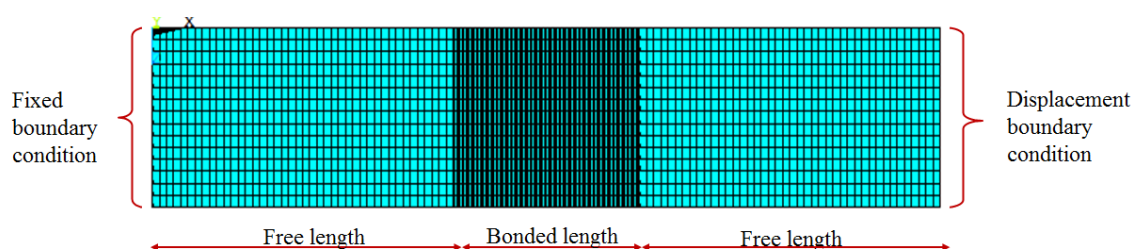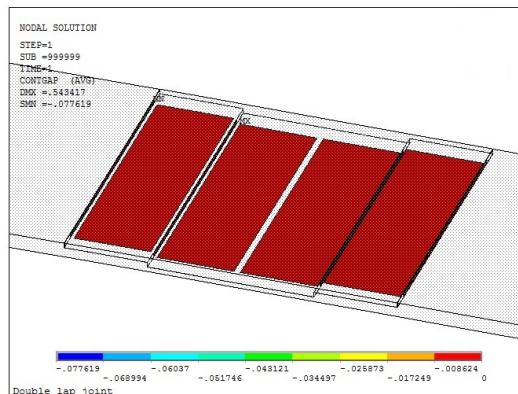

Figure 5.9: Finite element model of double stepped lap joint of CFRP panel

Table 5.5: Mesh parameters for double stepped lap joint of CFRP panel

Dimension	Number of elements
Free length	58
Step length	26
Width	30
Step height	4

5.3.4 Results and discussion

Local behaviour:

(a) Initial contact gap
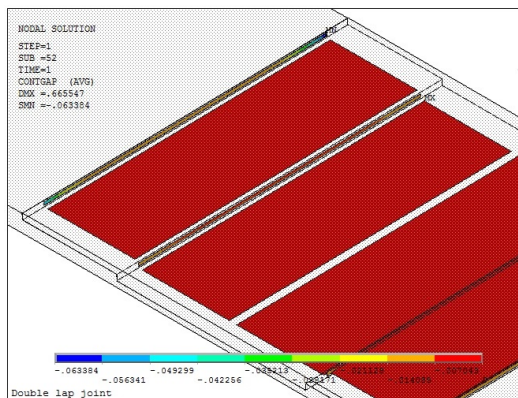
(b) Delamination propagation along step height
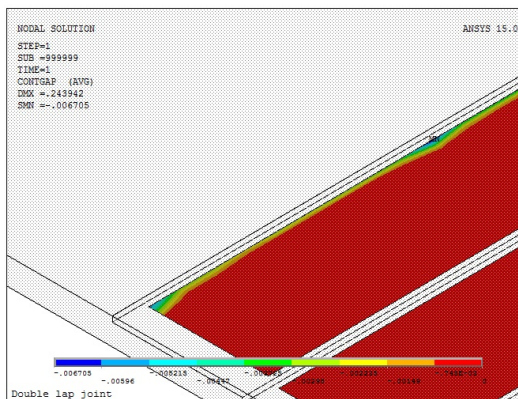
(c) Delamination propagation along step length

Figure 5.10: Contact gap distance for double stepped lap joint of CFRP panel

The Fig. 5.10 shows the contact gap distance for double stepped lap joint of CFRP panel. In the figure, (a) represents the initial contact gap and red region represents the contact distance of 0. Initially contact and target surfaces are bonded together. (b) represents the delamination propagation along step height. The delamination process starts at the step height. Step height

corners are separated initially and delamination propagates towards the centre of step. (c) represents the delamination along step length. After completion of delamination at step height, delamination starts along the length. In the length direction, delamination starts on the upper steps and then grows towards the central step. The onset point is 0.0027 mm and the region indicating green-blue area is already separated.
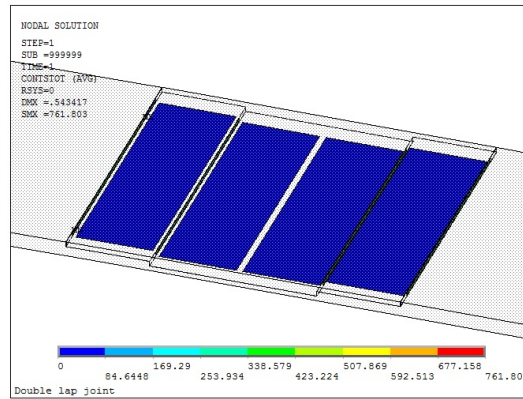
(a) Initial contact stress

(b) Contact stress along step height
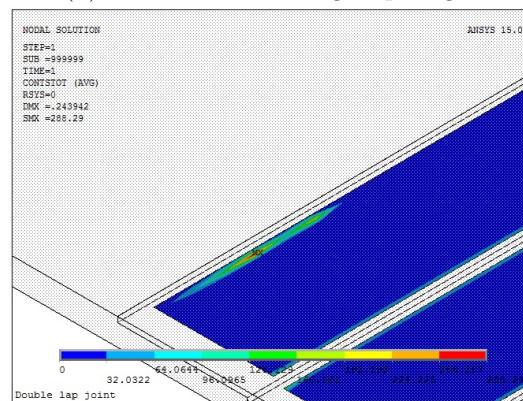
(c) Contact stress along step length

Figure 5.11: Contact stress for double stepped lap joint of CFRP panel

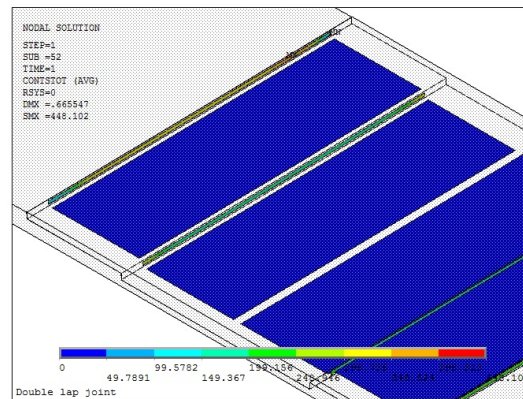The Fig. 5.11 shows the contact stress for double stepped lap joint of CFRP panel. In the figure,

(a) represents initial contact stress which is 0 and it indicates bonded region. (b) represents the contact stress along step height. The red region at the step corners corresponds to maximum stress and separation starts from corners and travels towards centre. (c) represents the contact stress along step length. At both the ends of step length, light blue region is observed indicating the start of the delamination process. The maximum stress is observed at the upper steps and it travels from upper step to central step.

Global behaviour:

The load-displacement curve is obtained as shown in the Fig 5.12. The load transfer between the adherends is by shear deformation mechanism. The failure starts near the first step corners on both the sides and then propagates towards the central step. Ultimate failure of the CFRP layer occurs along the adhesive layer.
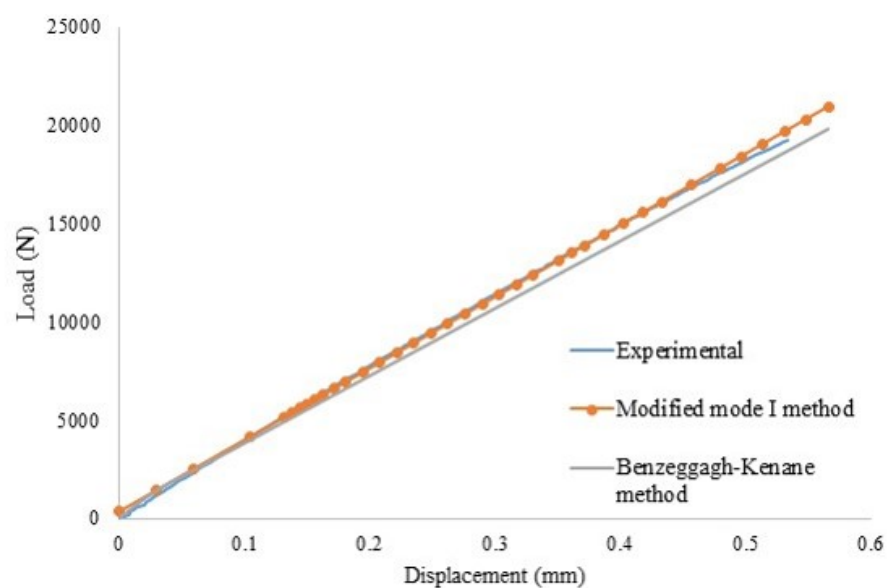
Figure 5.12: Load-displacement curve for double stepped lap joint of CFRP panel using contact modelling

5.4   Summary

In this chapter, experimental analysis of single and double stepped lap joint of CFRP panel under tensile loading is carried out. The load transfer between the adherends is by shear deformation mechanism. The failure starts near the step corners and then propagates towards the centre of the step. Ultimate failure of the CFRP panel occurs along the adhesive layer and panel splits into two. Load-displacement data obtained by experiment and modified modified mode I cohesive law show good match. Benzeggagh-Kenane method shows little deviation from experimental method. The material characterisation is performed for DCB specimen using numerical method which may not give accurate results. To get accurate results using B-K law, material parameter should be calibrated using experiments.

Chapter 6

Conclusion and future scope

6.1 Conclusion

In present work is focused on the analysis of single stepped lap joint of CFRP panel under tensile loading condition. Benzeggagh and Kenane formulation for mixed mode delamination is used to predict the debonding using contact pair modelling in ANSYS 15.

UserCZM found to capture the debonding mechanism of the panel accurately. The cohesive zone law is derived based on the static loading of the CFRP panels. To get mode I fracture toughness of an interface DCB test is carried out. For calculation of fracture toughness compliance calibration method with equivalent crack is used and the value obtained is 0.44 N/mm. For cohesive law characterisation the method used by Moura is followed. But the limitation involved is it cannot predict the onset of the delamination accurately. To get the onset of delamination whole field displacement obtained from DIC is used. By comparing the displacement and strain data, onset of delamination is obtained and initial stiffness is calculated. This completes the calibration of mode I cohesive law. For mode II fracture toughness calculation ENF test is used as recommended by ASTM D7905. For calculation of fracture toughness compliance calibration method is used and the value obtained is 2.76 N/mm. For mode II cohesive law characterisation various simulations are performed with varying traction-separation values at constant fracture toughness value. The load displacement curve for numerical method is matched with experiments to get the exact values of maximum shear traction and shear separation.

The main objective deals with the implementation of Benzeggagh and Kenane criteria for delamination. As the delamination process involves mode-mixity, mixed mode formulation is required. The Benzeggagh and Kenane criteria involves the characterisation of characteristic parameter of material, η. The parameter is obtained by performing various simulations with different η values. Numerical load-displacement curve for DCB specimen is matched with experimental curve. The match is obtained for the value $\eta = 3$.

The cohesive zone parameters obtained by above method are used in UserCZM. Analysis of single sided stepped lap joint of CFRP laminate under tensile loading is carried out. Experimental results are compared with numerical estimates and good match between load-displacement curve is obtained. The limitations involved in the process are: it is very time consuming and it requires high

computational power. The law is validated for static loading condition but its application for fatigue loading is still under question.

6.2 Suggestions for future work

It is observed that the present work can predict interface delamination failure in CFRP composites under static loading condition. The model can be extended to predict delamination failure under fatigue loading of constant amplitude.

References

[1] R. Campilho, M. de Moura, and J. Domingues. Using a cohesive damage model to predict the tensile behaviour of CFRP single-strap repairs. *International Journal of Solids and Structures* 45, (2008) 1497–1512.

[2] L. Hamitouche, M. Tarfaoui, and A. Vautrin. An interface debonding law subject to viscous regularization for avoiding instability: Application to the delamination problems. *Engineering Fracture Mechanics* 75, (2008) 3084 – 3100.

[3] V. K. Goyal. Analytical modeling of the mechanics of nucleation and growth of cracks. Ph.D. thesis, Virginia polytechnic institute and state university 2002.

[4] A. T. Travesa. Simulation of delamination in composites under quasi-static and fatigue loading using cohesive zone models. Ph.D. thesis, Universitat de Girona 2006.

[5] A. Turon, P. Camanho, J. Costa, and C. Davila. A damage model for the simulation of delamination in advanced composites under variable mode loading. *Mechanics of Materials* 38, (2006) 1072–1089.

[6] V. N. Burlayenko and T. Sadowski. FE modeling of delamination growth in interlaminar fracture specimens. *Budownictwo i Architektura* 2, (2008) 95–109.

[7] J. J. Munoz, U. Galvanetto, and P. Robinson. On the numerical simulation of fatigue drivendelamination with interface elements. *International Journal of Fatigue* 28, (2006) 1136–1146. The Third International Conference on Fatigue of CompositesThe Third International Conference on Fatigue of Composites.

[8] W. Ji and A. M. Waas. Progressive failure analysis for the interaction of interlaminar and intralaminar failure modes in composite structures with an initial delamination. *The Aeronautical Journal* 117, (2013) 71–85.

[9] T. L. Anderson. Fracture Mechanics: Fundamentals and applications. Taylor and Francis group, 2011.

[10] A. Needleman. Micromechanical modeling of interfacial decohesion. *Ultramicroscopy* 40, (1992) 203–214.

[11] X.-P. Xu and A. Needleman. Numerical simulations of fast crack growth in brittle solids. *Journal of the Mechanics and Physics of Solids* 42, (1994) 1397 – 1434.

[12] P. H. Geubelle and J. S. Baylor. Impact-induced delamination of composites: a 2D simulation. *Composites Part B: Engineering* 29, (1998) 589 – 602.

[13] G. Camacho and M. Ortiz. Computational modelling of impact damage in brittle materials. *International Journal of Solids and Structures* 33, (1996) 2899 – 2938.

[14] M. van den Bosch, P. Schreurs, and M. Geers. An improved description of the exponential Xu and Needleman cohesive zone law for mixed mode decohesion. *Enginnering Fracture Mechanics* 73, (2006) 1220–1234.

[15] V. Tvergaard and J. W. Hutchinson. The relation between crack growth resistance and fracture process parameters in elastic-plastic solids. *Journal of the Mechanics and Physics of Solids* 40, (1992) 1377 – 1397.

[16] M. Crisfield, G. Jelenic, Y. Mi, H.-G. Zhong, and Z. Fan. Some aspects of the non-linear finite element method. *Finite Elements in Analysis and Design* 27, (1997) 19–40.

[17] Y. Mi, M. Crisfield, G. Davies, and H. Hellweg. Progressive delamination using interface elements. *Journal of composite materials* 32, (1998) 1246–1272.

[18] T. Chen, B. Wang, Z. Cen, and Z. Wu. A symmetric Galerkin multi-zone boundary element method for cohesive crack growth. *Engineering fracture mechanics* 63, (1999) 591–609.

[19] Q. Yang and M. Thouless. Mixed-mode fracture analyses of plastically-deforming adhesive joints. *International Journal of Fracture* 110, (2001) 175–187.

[20] J. Li and J. K. Sen. Analysis of frame-to-skin joint pull-off tests and prediction of the delamination failure. *American institute of aeronautics and aeronautics* .

[21] Z. Qian and A. Akisanya. An investigation of stress singularity near the free edge of scarf joints. *European Journal of Mechanics - A/Solids* 18, (1998) 443–463.

[22] Z. Qian and A. Akisanya. An experimental investigation of failure initiation in bonded joints. *Acta Materialia* 46, (1998) 4895 – 4904.

[23] R. D. Campilho, M. De Moura, and J. Domingues. Modelling single and double-lap repairs on composite materials. *Composites Science and Technology* 65, (2005) 1948–1958.

[24] M. Benzeggagh and M. Kenane. Measurement of mixed-mode delamination fracture toughness of unidirectional glass/epoxy composites with mixed mode bending apparatus. *Composites science and technology* 56, (1995) 439–449.

[25] L. J. Hart-smith. Adhesively bonded scarf and stepped-lap joints.

[26] J. R. Rice. A Path Independent Integral and the Approximate Analysis of Strain Concentration by Notches and Cracks. *Journal of Applied Mechanics* 35, (1968) 379–386.

[27] A. D 5528-94a. Standard Test Method for Mode I Interlaminar Fracture Toughness of Unidirectional Fiber-Reinforced Polymer Matrix Composites. Technical Report, ASTM 1994.

[28] A. D 7905-14. Standard Test Method for Mode II Interlaminar Fracture Toughness of Unidirectional Fiber-Reinforced Polymer Matrix Composites. Technical Report, ASTM 1994.

[29] A. D 6671-01. Standard Test Method for mixed mode I- modeII Interlaminar Fracture Toughness of Unidirectional Fiber-Reinforced Polymer Matrix Composites. Technical Report, ASTM 2004.

[30] R. Harilal, C. Vyasarayani, and M. Ramji. A linear least squares approach for evaluation of crack tip stress field parameters using DIC. *Optics and Lasers in Engineering* 75, (2015) 95–102.

[31] G. Dias, M. de Moura, J. Chousal, and J. Xavier. Cohesive laws of composite bonded joints under mode I loading. *Composite Structures* 106, (2013) 646–652.